Bioorganic & Medicinal Chemistry 19 (2011) 4460–4472

Contents lists available at ScienceDirect

Bioorganic & Medicinal Chemistry

journal homepage: www.elsevier.com/locate/bmc

Design, synthesis and evaluation of *N*-benzoylindazole derivatives and analogues as inhibitors of human neutrophil elastase

Letizia Crocetti [a], Maria Paola Giovannoni [a,*], Igor A. Schepetkin [b], Mark T. Quinn [b], Andrei I. Khlebnikov [c], Agostino Cilibrizzi [a], Vittorio Dal Piaz [a], Alessia Graziano [a], Claudia Vergelli [a]

[a] *Dipartimento di Scienze Farmaceutiche, Università degli Studi di Firenze, Via Ugo Schiff 6, 50019 Sesto Fiorentino, Italy*
[b] *Department of Immunology and Infectious Diseases, Montana State University, Bozeman, MT 59717, USA*
[c] *Department of Chemistry, Altai State Technical University, Barnaul 656038, Russia*

ARTICLE INFO

Article history:
Received 28 February 2011
Revised 10 June 2011
Accepted 13 June 2011
Available online 7 July 2011

Keywords:
Indazoles
1-Benzoylindazoles
Human neutrophil elastase
Inhibitors
Structure–activity relationship

ABSTRACT

Human neutrophil elastase (HNE) plays an important role in tumour invasion and inflammation. A series of *N*-benzoylindazoles was synthesized and evaluated for their ability to inhibit HNE. We found that this scaffold is appropriate for HNE inhibitors and that the benzoyl fragment at position 1 is essential for activity. The most active compounds inhibited HNE activity with IC_{50} values in the submicromolar range. Furthermore, docking studies indicated that the geometry of an inhibitor within the binding site and energetics of Michaelis complex formation were key factors influencing the inhibitor's biological activity. Thus, *N*-benzoylindazole derivatives and their analogs represent novel structural templates that can be utilized for further development of efficacious HNE inhibitors.

1. Introduction

Human neutrophil elastase (HNE) is a member of the chymotrypsin superfamily of serine proteases and is expressed primarily in neutrophils.[1] It is a small, soluble protein of about 30 kDa, containing 218 amino acid residues and is stabilized by four disulfide bridges.[2] HNE is a basic glycoprotein, with a catalytic triad consisting of Ser195, His57, and Asp102.[3] HNE efficiently degrades a variety of extracellular matrix proteins, such as elastin, fibronectin, collagen, proteoglycans and laminin.[4] HNE also activates some matrix metalloproteinases (i.e., MMP-2, MMP-3 and MMP-9)[5] and is able to modulate cytokine expression and growth factors.[6,7] Under physiological conditions and during inflammation, endogenous HNE inhibitors, such as α_1-antitrypsin and elafin, protect tissues from damage by elastase.[8,9]

Several pathological conditions are known to result from imbalance between HNE and its endogenous inhibitors. In fact, HNE is considered to be the primary source of tissue damage associated with some inflammatory diseases, such as adult respiratory distress syndrome (ARDS),[10] chronic obstructive pulmonary disease (COPD),[11] cystic fibrosis (CF),[12] and other inflammatory disorders.[13–15] Massive HNE release can also contribute to the movement of neoplastic cells through tissues.[16] Thus, it is clear that agents able to modulate the proteolytic activity of HNE represent promising therapeutics for pathological conditions involving excessive HNE activity.[17]

Over the past two decades, intensive research has resulted in the development of a number of HNE inhibitors, including peptidic and non-peptidic compounds, some of which have been tested in clinical trials.[18–22] More recently, low molecular weight HNE inhibitors have appeared in literature,[21–29] and examples of different structural classes of these inhibitors are shown in Figure 1. Among these, the 2-pyridin-3-yl-benzo[*d*]1,3-oxazin-4-ones (structure **A**) exhibited a very good balance of potency (K_i = 28 nM) and stability ($t_{1/2} \sim$ 23.3 h at pH 9.2),[28] the 3,3-diethyl-1-(4-tolyl)azetidine-2,4-diones (structure **B**), had K_i values in the low micromolar range and acted as an irreversible inhibitors of elastase,[26] and the *N*-benzoylpyrazoles (structure **C**) were potent, competitive, pseudoirreversible inhibitors of HNE with K_i values in the nanomolar range.[23] However, despite the numerous inhibitors described in the literature, the only small-molecule HNE inhibitor currently available for clinical use is Sivelestat (ONO-5046), which is marketed in Japan and Korea.[30] ONO-5046 is a competitive and selective inhibitor of HNE and is used for the treatment of acute lung injury (ALI) associated with systemic inflammatory response syndrome (SIRS).[31]

Based on previous studies showing that *N*-benzoylpyrazoles were potent HNE inhibitors,[23] we synthesized a series of *N*-benzoylindazoles (Fig. 1, structure **D**), which build upon the basic pyrazole feature (structure **C**) by linking the benzoyl fragment to the

* Corresponding author. Tel.: +39 055 4573682; fax: +39 055 4573780.
E-mail address: mariapaola.giovannoni@unifi.it (M.P. Giovannoni).

0968-0896/$ - see front matter © 2011 Elsevier Ltd. All rights reserved.
doi:10.1016/j.bmc.2011.06.036

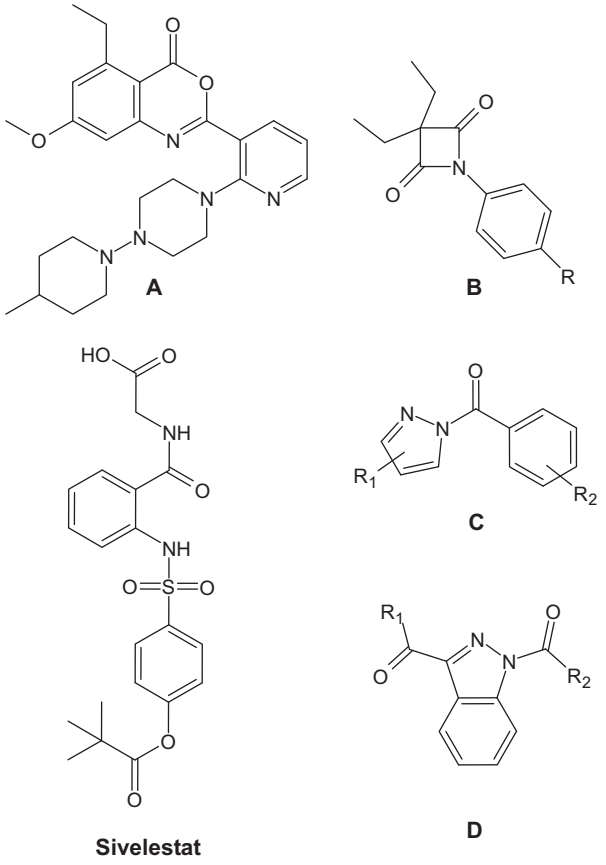

Figure 1. Structures of selected HNE inhibitors.

cyclic amide, and evaluated these compounds and various derivatives for their ability to inhibit HNE. We also utilized molecular modelling to evaluate binding of the compounds to the HNE active site and obtained insight into the differences in inhibitory activity of the various derivatives.

2. Chemistry

We followed a simple synthetic route that allowed us to obtain a large number of 1-aroylindazole derivatives and to obtain preliminary information about the structural requirements for the activity of this new scaffold.

The synthesis of all compounds bearing an aroyl fragment [compounds **3a**–**q**, **5a**–**s** (**5a**,[32] **5b**–**k**[33]), and **8a**–**p**] or an acyl fragment [compounds **6a**–**e** (**6a**[32])] at position 1 of the indazole nucleus is depicted in Scheme 1, and the final products are grouped into the **3**, **5**, **6** or **8** series in order to facilitate discussion of the pharmacological results. Using previously described conditions, we first transformed the commercially available indazole-3-carboxylic acid **1** into the corresponding phenylamide **2**[34] and the known esters **4**[32] and **7a**–**c**.[35] The novel **7d** was prepared from a reaction of **1** with trifluoroethanol *via* the acid chloride. Introduction of the acyl function at N-1 of various indazoles was performed following three different approaches, as follows: (1) treating the appropriate aroyl or acyl chloride, where commercially available, with dichloromethane and triethylamine; (2) preparing the appropriate aroyl chloride starting from the corresponding acid and then carrying out the reaction in anhydrous toluene and triethylamine; and (3) coupling with the appropriate acid in dimethylformamide (DMF) by treatment with triethylamine and diethylcyanophosphonate (DCF). Compounds **3**, **5**, **6** and **8** are defined in Tables 1–3.

When the benzoyl fragment at position 1 was substituted at the *meta* position with an amino group, it was necessary to protect the NH_2 function of **9** with di-terbutyldicarbonate to obtain the intermediate **10**[36] (Scheme 2). This compound was treated with ethyl chloroformate in anhydrous tetrahydrofuran (THF) in the presence of trietylamine, resulting in the mixed anhydride **11**, which was reacted with the appropriate indazole to give compounds **12a**–**f**. The last step was removal of the protecting group by using triofluoroacetic acid and dichloromethane.

Scheme 3 depicts the synthetic route which, starting from the precursors **2** and **4**, allowed us to modify the amidic function at position 1 by inserting a sulphonamidic moiety (**14a**,**b**), replacing the CO group with a CH_2 (**14c**), eliminating the CO between N-1 and phenyl ring (**14d**), inserting a methylenic spacer between N-1 and CO (**14e**), and finally introducing a CONH fragment (**14f**,**g**). The sulphonamide derivatives **14a**,**b** were obtained by treatment with the desired sulphonyl chloride in dichloromethane and triethylamine; compounds **14c** and **14e** were synthesized using the appropriate benzyl or phenacyl halides in anhydrous solvent and K_2CO_3; synthesis of derivative **14d** was performed through a cross-coupling reaction with 4-chlorophenylboronic acid, using copper acetate as catalyst and a weak base (triethylamine) in dichloromethane; and treatment of **4** with substituted phenyl isocyanate in anhydrous THF afforded the semicarbazone derivatives **14f**,**g**.

Scheme 4 depicts the synthetic routes followed to obtain **17a**,**b** and **19a**,**b**, where the function at position 3 was replaced with a methyl group (**17a**,**b**), a carboxylic group (**19b**), or a hydrogen (**19a**). Treatment of the commercially available *o*-bromoacetophenone **15** with hydrazine hydrate at high temperature afforded the 3-methylindazole **16**,[37] which was transformed into the final compounds **17a**,**b**, as reported in Scheme 1. Following the same procedure, final product **19a**[38] was synthesized. Finally, treatment of compound **5c** with 6 N NaOH at 60 °C afforded **19b**.

3. Biological results and discussion

3.1. Structure–activity relationship analysis

All compounds were evaluated for their ability to inhibit HNE, and the results are presented in Tables 1–5. The first compounds synthesized were the 3-phenylamido (**3a**–**q**, **13a**) and 3-carbethoxy (**5a**–**s**, **13b**) derivatives (Table 1). Compounds **3a** and **5a**, bearing an unsubstituted benzoyl group at position 1, exhibited submicromolar inhibitory activity (IC_{50} = 0.4 μM). This suggested that the 1-benzoylindazole system could represent a suitable scaffold for HNE inhibitors. Thus, as a primary approach, we modified the benzoyl fragment. Introduction of a methyl (**3b** and **5b**) or a chlorine (**3e** and **5e**) at the *ortho* position of the phenyl ring led to decreased activity for both series of compounds. In particular, compounds **3b** and **5b** had 3 orders of magnitude lower activity compared to **3a** and **5a** (IC_{50} = 34 and 52 μM, respectively), whereas **3e** and **5e** were completely devoid of activity, suggesting that the *ortho* position has to remain unsubstituted to permit free rotation, which is in agreement with that reported for the pyrazoles (see Fig. 1, structure **C**).[23]

The introduction of substituents in the *para* position resulted in variable effects on HNE inhibitory activity. For example, the *p*-methyl (**3d** and **5d**) and the 4-CN (**3m** and **5m**) derivatives were only weak inhibitors, both for the phenylamide and carbethoxy series (IC_{50} = 29 and 36 μM, respectively). In contrast, compounds **3i** and **5i**, both bearing a 4-NO_2 group, were completely inactive. The 4-Cl (**3g** and **5g**) and the 4-F-benzoyl (**3k** and **5k**) derivatives were the only products that retained inhibitory activity, although still lower when compared to the unsubstituted reference

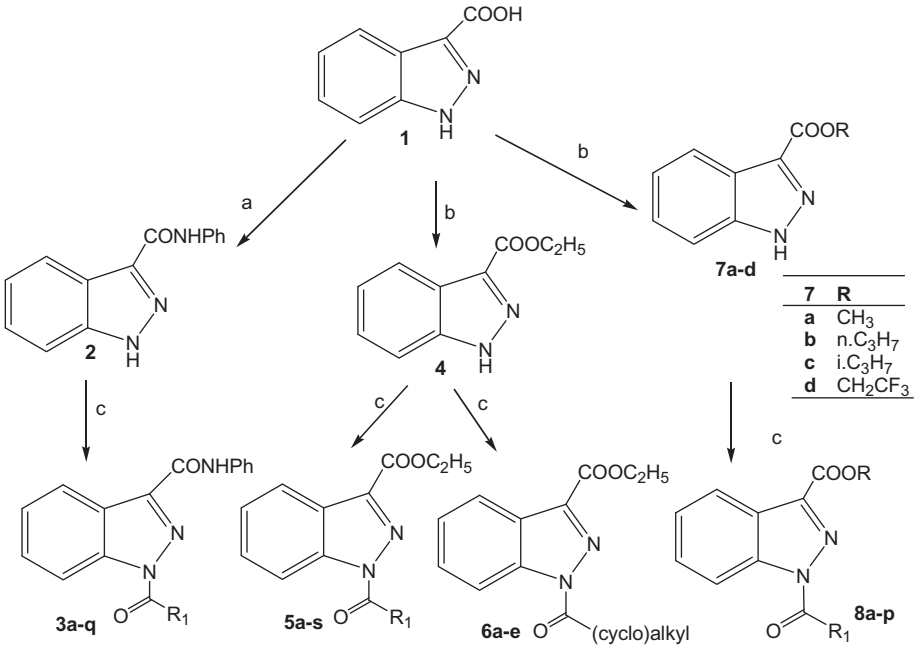

Scheme 1. Synthesis of indazoles **3a–q**, **5a–s**, **6a–e** and **8a–p**. *Reagents and conditions:* (a) $SOCl_2$, Et_3N, THF, $PhNH_2$, 0 °C–rt; (b) for **4**, **7a–c**: ROH, H_2SO_4, reflux; for **7d**: $SOCl_2$, Et_3N, CF_3CH_2OH, dry toluene, rt; (c) for **3a–k**, **3m** and **3q**, **5a–k**, **5m**, **5q** and **5r**, **6b–c** and **6e**, **8a–b**, **8e–f**, **8i–j** and **8m–n**: aroylchloride, Et_3N, DCF, dry CH_2Cl_2, 0 °C–reflux; for **3l** and **3o–p**, **5l** and **5o–p**: (hetero)aryl carboxylic acid, Et_3N, DCF, dry DMF, rt; for **3n**, **5n** and **5s**, **6d**, **8g–h**, **8k–l**, **8o–p**: (ethero)aryl carboxylic acid, $SOCl_2$, Et_3N, dry toluene, reflux.

Table 1
HNE inhibitory activity of indazole derivatives **3a–q**, **5a–s**, and, **13a**,**b**

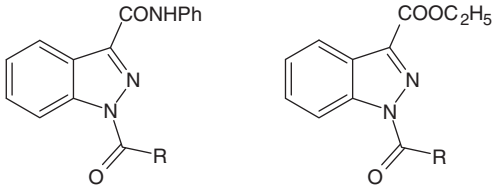

3a-q, 13a **5a-s, 13b**

R	Compound	IC_{50} (μM)[a]	Compound[b]	IC_{50} (μM)[a]
Ph	**3a**	0.42 ± 0.21	**5a**[32]	0.40 ± 0.19
2-CH_3Ph	**3b**	34 ± 5.2	**5b**[33]	52 ± 7.3
3-CH_3Ph	**3c**	0.93 ± 0.30	**5c**[33]	0.41 ± 0.11
4-CH_3Ph	**3d**	29 ± 4.8	**5d**[33]	36 ± 4.9
2-ClPh	**3e**	NA	**5e**[33]	NA
3-ClPh	**3f**	3.9 ± 1.6	**5f**[33]	1.7 ± 0.61
4-ClPh	**3g**	6.1 ± 2.4	**5g**[33]	19 ± 4.1
3-NO_2Ph	**3h**	11 ± 3.8	**5h**[33]	NA
4-NO_2Ph	**3i**	NA	**5i**[33]	NA
3-FPh	**3j**	5.9 ± 2.1	**5j**[33]	1.7 ± 0.52
4-FPh	**3k**	8.1 ± 3.2	**5k**[33]	5.7 ± 2.3
3-OCH_3Ph	**3l**	1.8 ± 0.71	**5l**	0.80 ± 0.33
4-CNPh	**3m**	38 ± 5.3	**5m**	38 ± 4.7
4-Pyridyl	**3n**	NA	**5n**	NA
3-Thienyl	**3o**	3.1 ± 1.1	**5o**	0.93 ± 0.37
5-Benzodioxole	**3p**	33 ± 4.6	**5p**	28 ± 3.4
1-Naphthyl	**3q**	25 ± 3.9	**5q**	NA
3-CF_3Ph	—		**5r**	NA
3,4,5-OCH_3Ph	—		**5s**	NA
3-NH_2Ph	**13a**	3.1 ± 1.2	**13b**	1.6 ± 0.58

NA, no activity was observed at concentrations below 55 μM.
[a] The IC_{50} values are presented as the mean ± SD of three independent experiments.
[b] References for previously reported compounds are indicated.

Table 2
HNE inhibitory activity of indazole derivatives **8a–p** and **13c–f**

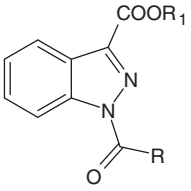

Compound	R	R_1	IC_{50} (μM)[a]
8a	Ph	CH_3	0.089 ± 0.031
8b	3-CH_3Ph	CH_3	0.13 ± 0.051
8c	3-OCH_3Ph	CH_3	0.55 ± 0.21
8d	3-Thienyl	CH_3	0.31 ± 0.12
13c	3-NH_2Ph	CH_3	NA
8e	Ph	nC_3H_7	0.40 ± 0.18
8f	3-CH_3Ph	nC_3H_7	0.78 ± 0.32
8g	3-OCH_3Ph	nC_3H_7	1.9 ± 0.78
8h	3-Thienyl	nC_3H_7	1.9 ± 0.72
13d	3-NH_2Ph	nC_3H_7	0.70 ± 0.26
8i	Ph	iC_3H_7	0.24 ± 0.088
8j	3-CH_3Ph	iC_3H_7	0.65 ± 0.28
8k	3-OCH_3Ph	iC_3H_7	0.76 ± 0.34
8l	3-Thienyl	iC_3H_7	0.69 ± 0.31
13e	3-NH_2Ph	iC_3H_7	0.51 ± 0.24
8m	Ph	CH_2CF_3	0.26 ± 0.11
8n	3-CH_3Ph	CH_2CF_3	0.46 ± 0.21
8o	3-OCH_3Ph	CH_2CF_3	0.89 ± 0.37
8p	3-Thienyl	CH_2CF_3	0.51 ± 0.23
13f	3-NH_2Ph	CH_2CF_3	0.34 ± 0.13

NA, no activity was observed at concentrations below 55 μM.
[a] The IC_{50} values are presented as the mean ± SD of three independent experiments.

compounds **3a** and **5a** (**3g**, IC_{50} = 6.1 μM; **5g**, IC_{50} = 19 μM; **3k**, IC_{50} = 8.1 μM; **5k**, IC_{50} = 5.7 μM). Moreover, the 4-Cl derivatives exhibited different activity in the two series, where **3g** was about 3 times more potent than **5g**.

When substituents were introduced at the *meta* position of the benzoyl group, the most active products were the 3-methyl and 3-methoxy derivatives, which had IC_{50} values similar to those of the

Table 3
HNE inhibitory activity of indazole derivatives **6a–e**

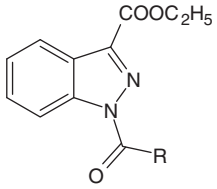

Compound[a]	R	IC_{50} (μM)[b]
6a[32]	CH_3	4.8 ± 1.9
6b	C_2H_5	0.40 ± 0.18
6c	nC_3H_7	0.18 ± 0.068
6d	Cyclopentyl	0.48 ± 0.19
6e	Cyclohexyl	NA

NA, no activity was observed at concentrations below 55 μM.
[a] References for previously reported compounds are indicated.
[b] The IC_{50} values are presented as the mean ± SD of three independent experiments.

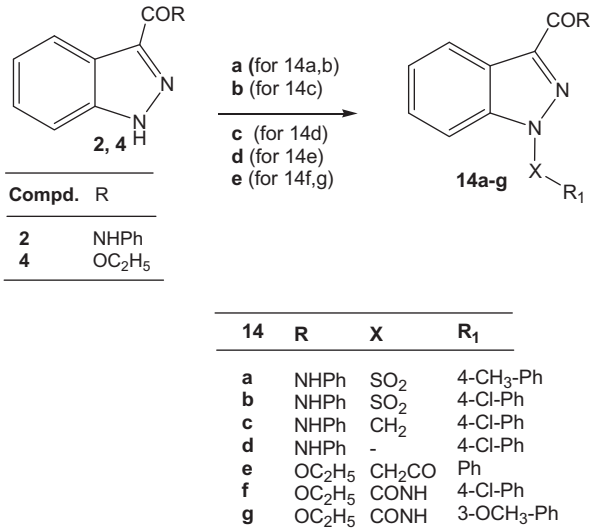

Compd.	R
2	NHPh
4	OC_2H_5

14	R	X	R_1
a	NHPh	SO_2	4-CH_3-Ph
b	NHPh	SO_2	4-Cl-Ph
c	NHPh	CH_2	4-Cl-Ph
d	NHPh	-	4-Cl-Ph
e	OC_2H_5	CH_2CO	Ph
f	OC_2H_5	CONH	4-Cl-Ph
g	OC_2H_5	CONH	3-OCH_3-Ph

Scheme 3. Synthesis of indazoles **14a–g**. *Reagents and conditions:* (a) Et_3N, appropriate sulfonylchloride, anhydrous CH_2Cl_2, rt; (b) 4-chlorfobenzylchloride, K_2CO_3, anhydrous DMF, 80 °C; (c) 4-chlorobenzeneboronic acid, $Cu(Ac)_2$, Et_3N, CH_2Cl_2, rt; (d) phenacylbromide, K_2CO_3, anhydrous acetone, rt; (e) appropriate phenylisocyanide, anhydrous THF, rt.

unsubstituted compounds. In particular, compounds **5c** and **5l** had IC_{50} values of 0.41 and 0.80 μM, respectively. Compounds bearing an amino group (**13a** and **13b**), a chlorine (**3f** and **5f**), or a fluorine (**3j** and **5j**) at the same position retained HNE inhibitory activity, but at lower levels (Table 1). In comparison, insertion of a nitro (**3h** and **5h**) or a trifluoromethyl group (**5r**) led to weak or inactive compounds. These results indicate that the presence of an electron-withdrawing group in this position is detrimental. The increased steric bulk due to the insertion of 3,4,5-OCH_3Ph led to a complete loss of activity (**5s**), as did replacement of the phenyl linked to CO at position 1 of the indazole nucleus with a heterocyclic ring, such as 4-pyridyl (**3n** and **5n**), 5-benzodioxole (**3p** and **5p**), or 1 naphtyl (**3p** and **5p**). The only exception was substitution with a 3-thienyl ring, which produced active compounds (**3o** and **5o**). In particular **5o**, belonging to the carbethoxy series, had an IC_{50} = 0.93 μM.

We next performed modifications of residue R_1 of the ester function in position 4, while maintaining at position R_2 the best substituent features determined above for each series (i.e., benzoyl, 3-methyl-benzoyl, 3-methoxy-benzoyl, 3-amino-benzoyl, and 3-thienyl) (see Table 2). Analysis of the biological activity of these compounds (**8a–p** and **13c–f**) demonstrated that HNE inhibitory activity improved by changing –COOEt to –COOMe, –COOnPr, –COOiPr, or $-COOCH_2CF_3$ (Table 2). In fact, for most compounds, these modifications resulted in increased HNE inhibitory activity (about one order of magnitude) with respect to the –COOEt derivatives. In particular, the –COOMe derivative **8a** was the most active in this series (IC_{50} = 89 nM). On the other hand, not all such derivatives were active, and the 3-amino derivative **13c** was completely inactive.

We also evaluated the effects of replacement of the ring with a (cyclo)alkyl fragment (compounds **6a–e**) (Table 3). The most active compound was **6c**, with R = nPr (IC_{50} = 0.18 μM). The activity of

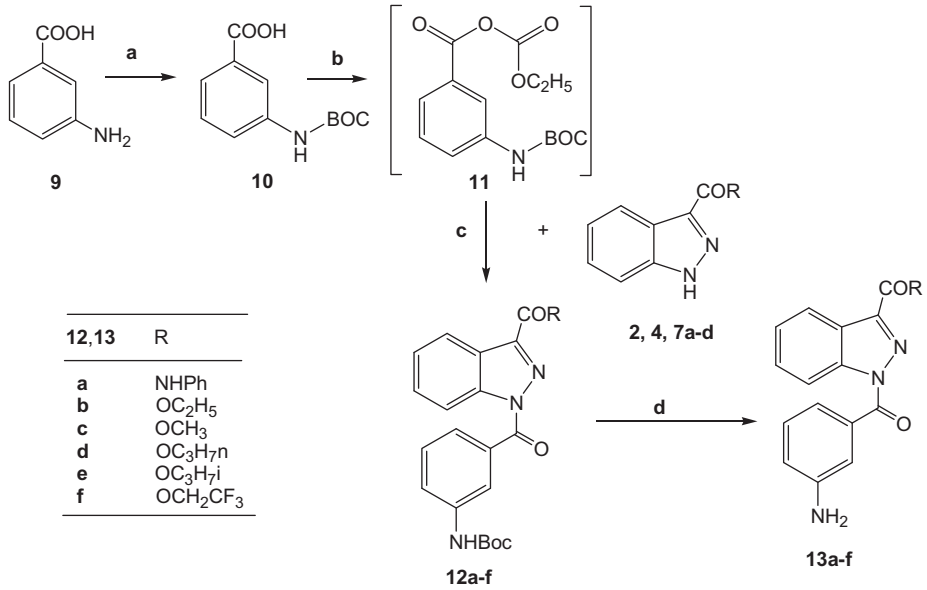

12,13	R
a	NHPh
b	OC_2H_5
c	OCH_3
d	OC_3H_7n
e	OC_3H_7i
f	OCH_2CF_3

Scheme 2. Synthesis of indazoles **13a–f**. *Reagents and conditions:* (a) $(BOC)_2O$, Et_3N, dioxane, H_2O, rt; (b) (1) Et_3N, dry THF-7 °C/-5 °C; (2) ClCOOEt, 0 °C; (c) rt–60 °C; (d) CH_2Cl_2, CF_3COOH, rt.

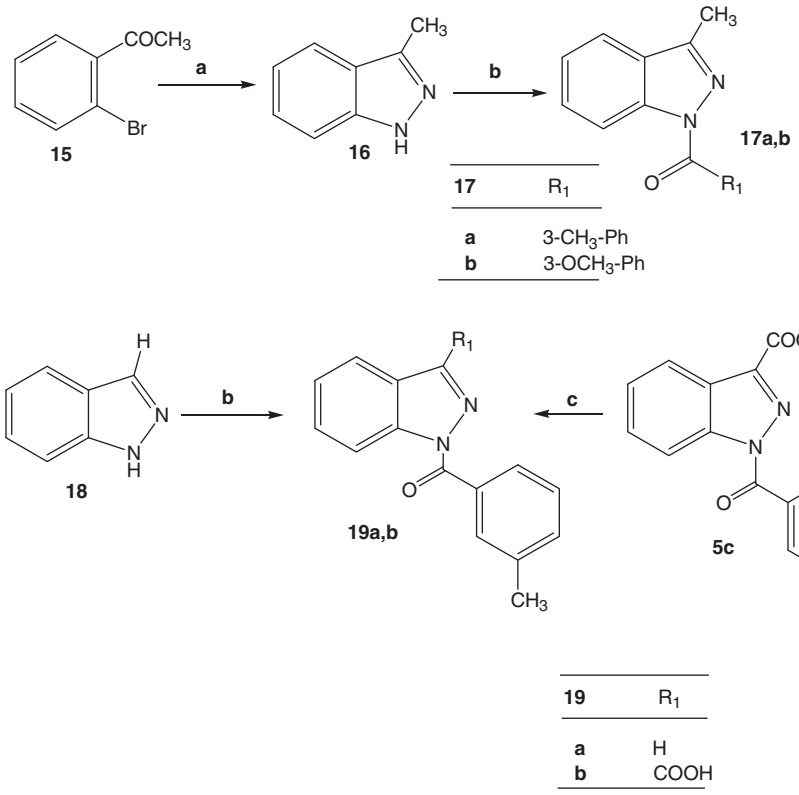

Scheme 4. Synthesis of indazoles **17a**,**b** and **19a**,**b**. *Reagents and conditions:* (a) $NH_2NH_2{\cdot}H_2O$, 120 °C; (b) for **17a** and **19a**: *m*-toluoyl chloride, Et_3N, anhydrous CH_2Cl_2, 0 °C–rt ; for **17b**: 3-methoxybenzoic acid, $SOCl_2$, Et_3N, anhydrous toluene, 100 °C; (c) 6 N NaOH, 60 °C.

Table 4
HNE inhibitory activity of indazole derivatives **14a**–**g**

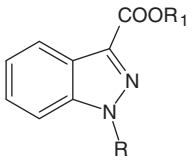

Compound	R	R_1	IC_{50} (μM)[a]
14a	4-CH_3-$PhSO_2$	NHPh	NA
14b	4-Cl-$PhSO_2$	NHPh	NA
14c	4-Cl-$PhCH_2$	NHPh	NA
14d	4-Cl-Ph	NHPh	NA
14e	$PhCOCH_2$	OC_2H_5	NA
14f	4-Cl-PhNHCO	OC_2H_5	NA
14g	3-OCH_3-PhNHCO	OC_2H_5	NA

[a] No activity was observed at concentrations below 55 μM.

Table 5
HNE inhibitory activity of indazole derivatives **17a**,**b** and **19a**,**b**

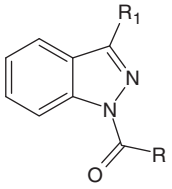

Compound[a]	R	R_1	IC_{50} (μM)[b]
17a	3-CH_3-Ph	CH_3	22 ± 6.8
17b	3-OCH_3-Ph	CH_3	NA
19a[38]	3-CH_3-Ph	H	10 ± 2.2
19b	3-CH_3-Ph	COOH	NA

NA, no activity was observed at concentrations below 55 μM.
[a] References for previously reported compounds are indicated.
[b] The IC_{50} values are presented as the mean ± SD of three independent experiments.

compounds in this series decreased both by shortening the alkylic chain (e.g., **6a** with R = Me was 10-fold less active than **6c**), and by increasing the bulk, as demonstrated by the complete inactivity of **6e** bearing a cyclohexyl group. These results suggest that a specific steric requirement is necessary at this position.

To consider the effects of modifications at the level of the amidic group, we synthesized a number of 3-phenylamide and 3-carbomethoxy derivatives. These modifications included replacement of the amidic CO with SO_2 (**14a**,**b**) or a methylenic linker (**14c**), bonding of the phenyl ring directly to the indazole by deletion of the amidic CO (compound **14d**), insertion of a methylenic spacer between the amidic nitrogen and the amidic CO (**14e**), and insertion of a CONH group (**14f**,**g**) (Table 4). In all cases, these modifications led to a complete loss of activity. These data demonstrate that the cyclic amidic function is essential for HNE inhibitory activity, suggesting that interaction with the enzyme is mediated by the nucleophilic attack at the amide carbonyl group. We also analyzed the importance of the ester function at position 3 of the indazole scaffold by hydrolyzing, removing, or replacing this feature with a methyl group. As shown in Table 5, these elaborations significantly affected inhibitory activity, resulting in inactive compounds (**17b** and **19b**) or weak inhibitors (**17a** and **19a**).

The most active *N*-benzoylindazole derivatives identified here ($IC_{50} \sim 90$–100 nM) are similar in HNE inhibitory activity to other currently reported small-molecule HNE inhibitors, such as Sivelestat (ONO-5046; IC_{50} = 44 nM),[30] Midesteine (MR889; IC_{50} = 1–10 μM),[39] and 2-pyridin-3-yl-benzoxazinone (IC_{50} = 61 nM).[40]

Table 6
Analysis of *N*-benzoylindazole inhibitory specificity

Compound	IC_{50} (μM)		
	Thrombin	Urokinase	Chymotrypsin
6c	5.2 ± 1.9	14 ± 3.5	0.43 ± 0.13
8a	14 ± 4.2	1.2 ± 0.028	0.081 ± 0.018
8b	5.1 ± 1.8	0.87 ± 0.33	0.030 ± 0.013
8d	NA	12 ± 4.2	0.26 ± 0.087
8i	7.8 ± 2.7	6.3 ± 2.1	0.047 ± 0.011
8m	6.7 ± 2.4	10 ± 3.1	0.0029 ± 0.0012

3.2. Specificity

To evaluate inhibitor specificity, we analyzed effects of the six most potent *N*-benzoylindazole derivatives on three other serine proteases, including human pancreatic chymotrypsin (EC 3.4.21.1), human thrombin (EC 3.4.21.5), and human urokinase (urokinase-type plasminogen activator precursor, EC 3.4.21.73). As shown in Table 6, most of selected compounds inhibited thrombin and urokinase at micromolar concentrations, whereas the derivatives were potent chymotrypsin inhibitors. This is not surprising, as HNE and chymotrypsin belong to same enzyme family, and several known HNE inhibitors are also relatively potent chymotrypsin inhibitors.[41,42]

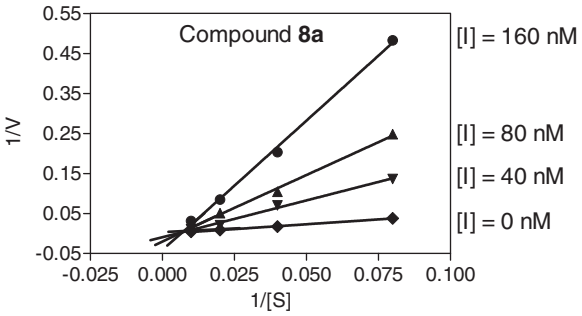

Figure 2. Kinetics of HNE inhibition by compound **8a**. Representative double-reciprocal Lineweaver–Burk plot from three independent experiments.

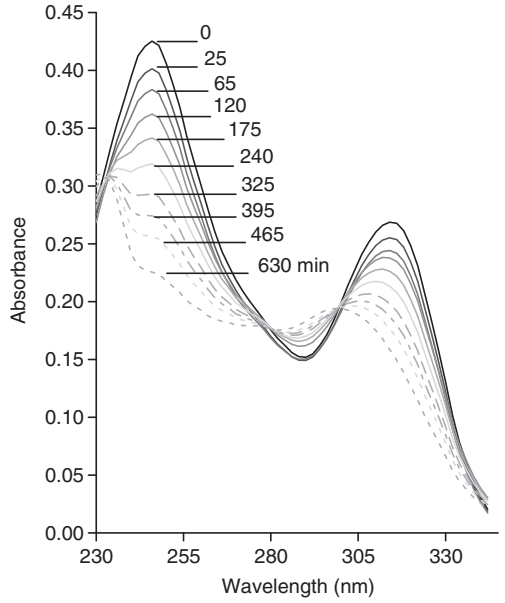

Figure 3. Analysis of spontaneous hydrolysis of *N*-benzoylindazole derivative **8a**. The change in absorbance spectrum of compound **8a** (20 μM in 0.05 M phosphate buffer, pH 7.3, 25 °C) was monitored over time in solution. Representative scans are from two independent experiments.

3.3. Kinetic features and stability

To better understand the mechanism of action of these compounds, we performed kinetic experiments with two of the most active compounds (**8a** and **8b**). As shown in Fig. 2, the representative double-reciprocal Lineweaver–Burk plot of fluorogenic substrate hydrolysis by HNE in the absence and presence of compound **8a** indicates that this compound is a competitive HNA inhibitor. Similar results were observed with kinetic analysis of compound **8b** (data not shown).

Compound **8a** was further evaluated for chemical stability in aqueous buffer using spectrophotometry to detect compound hydrolysis.[23] Fig. 3 shows that the absorbance maxima at 246 and 314 nm decreased over time, indicating that the compound was hydrolyzed almost completely after 10 h in aqueous buffer. This relatively rapid rate of spontaneous hydrolysis allowed us to evaluate reversibility of HNE inhibition over time. As shown in Fig. 4A, HNE was rapidly inhibited, with no lag period after addi-

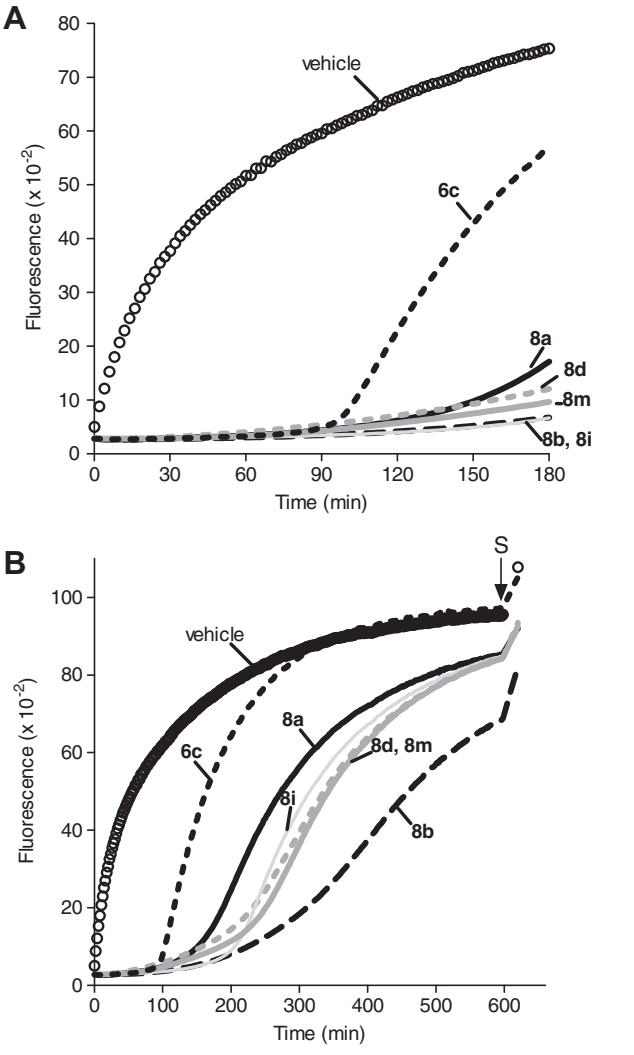

Figure 4. Evaluation of HNE inhibition by representative *N*-benzoylindazoles over extended periods of time. HNE was incubated with the indicated compounds (600 nM), and kinetic curves monitoring substrate cleavage catalyzed by HNE during the first 180 min (Panel **A**) and from 0 to 10 h (Panel **B**) are shown. The arrow indicates addition of additional fluorogenic substrate (S). Representative curves are from two independent experiments.

tion of compound, and inhibition was maximal during the first 90 min with compounds **6c** and 120 min with the other tested compounds (**8a**, **8b**, **8d**, **8m**, and **8i**). However, inhibition by compound **6c** was soon reversed, and full recovery of HNE activity was observed by ~5 h after treatment with up to 600 nM of the compound (Fig. 4B). In comparison, reversal of inhibition by **8a**, **8d**, **8m**, and **8i** was much slower, and HNE was still inhibited to 50% of control level by 600 nM of these compounds at 5 h after treatment (Fig. 4B). Furthermore, subsequent addition of more fluorogenic substrate showed that the enzyme was still active after the 10 h incubation period (indicated by arrow in Fig. 4B). Thus, these results suggest that the active *N*-benzoylindazoles may be pseudoirreversible inhibitors of HNE, which covalently attack the enzyme active site but can be reversed by hydrolysis of the acyl-enzyme complex, as discussed previously for structure-related *N*-benzoylpyrazole-derived HNE inhibitors.[23]

3.4. Molecular modelling

To investigate binding of compounds to the HNE active site and obtain insight into the differences in inhibitory activity of the various derivatives, we selected active and inactive compounds and performed molecular modelling studies using a 23-residue model of the HNE binding site, as described previously.[23] The binding site was derived from the 1.84 Å resolution crystal structure of HNE complexed with a peptide chloromethyl ketone inhibitor.[43] We imported this structure of the HNE binding site into ArgusLab and performed docking studies to identify binding modes of the flexible ligands that were favourable for the interaction between the hydroxyl group of Ser195 and the carbonyl group of the compounds under investigation. This approach is based on a number of reports showing that the mechanism of action of serine protease inhibitors containing an N–C=O fragment involves interaction between the inhibitor's carbonyl group and Ser195[44–46] and/or other targets in the active site.[42,47] This mechanism of interaction has been shown to involve formation of an intermediate Michaelis complex, where the inhibitor carbonyl carbon atom is located 1.8–2.6 Å from the Ser195 hydroxyl oxygen (distance d_1), while the angle of Ser195 O$\gamma\cdots$C=O, denoted as angle α, is limited to 80–120°[8,45,48] (Fig. 5).

The most favourable binding modes for six active (**5c**, **6c**, **8a**, **8b**, **8d**, and **13f**) and five inactive (**14b**, **14c**, **14d**, **17b**, and **19b**) compounds were chosen from ligand docking poses lying within a 2 kcal/mol energy gap above the lowest-energy binding mode for each compound. Representative binding modes for active **8a** and inactive **14d** are shown in Fig. 6. The d_1 and α values show that

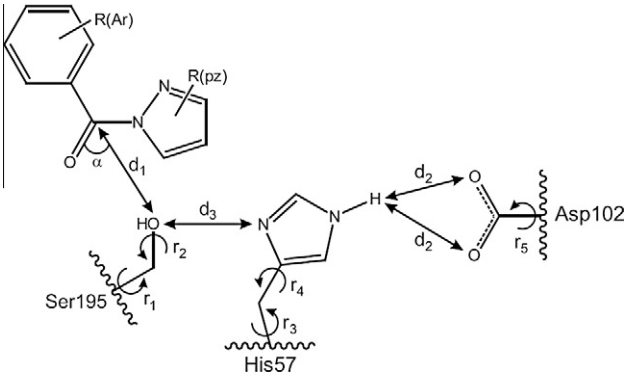

Figure 5. Geometric parameters important for formation of a Michaelis complex in the HNE active site. The important distances (d) and relevant angle (α), as specified in the text, are indicated. Based on the model of synchronous proton transfer from the oxyanion hole in HNE. Reproduced from Ref.[22]

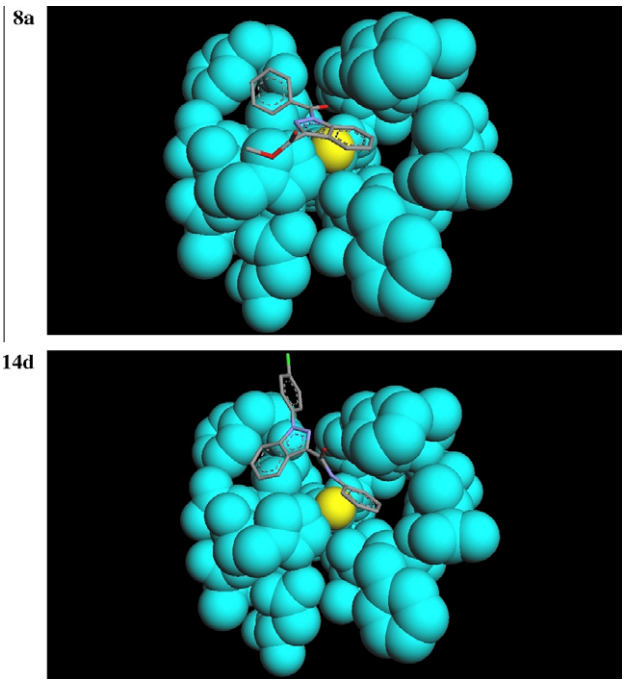

Figure 6. Molecular docking of active (**8a**) and inactive (**14d**) compounds into the binding site of HNE. The Ser195 hydroxyl oxygen is yellow. For the ligand structures, carbon is gray, hydrogen is white, nitrogen is violet, oxygen is red, and chlorine is green.

the carbonyl carbon atom is more accessible to the Ser195 hydroxyl oxygen in active compounds, as compared to inactive compounds (d_1 = 3.49 ± 0.47 versus 5.91 ± 1.01 Å, respectively) (Table 7). Docking poses for inactive compounds are characterized by remarkably obtuse angle α (148.4 ± 9.4), whereas this angle is 67.2 ± 4.1° for active indazole derivatives. Obviously, these geometric parameters strongly influence the ability of a molecule to form Michaelis complex and define energy of molecular distortion on the formation of such complex (see below).

Three residues, Ser195, His57, and Asp102, form an active site triad that catalyzes synchronous proton transfer from Ser195 to Asp102, with His57 acting as a general base to enhance nucleophilicity of the Ser195 hydroxyl oxygen and activate the hydrolytic H_2O[23,43,49,50] (Fig. 2). While rotational lability of the catalytic triad residues could result in a more favourable environment for substrate binding and cleavage, certain rotational freedom could also destroy the conformationally sensitive 'channel' of proton migration during formation of the Michaelis complex. To explore this issue, five torsion angles (r_1–r_5) in Ser195, His57, and Asp102 (Fig. 2) were varied during optimization with the MM+ force field, while concurrently applying harmonic restraints to d_1 and α, as described previously.[23] This approach allowed us to evaluate if rotational flexibility in Ser195, His57, and Asp102 could lead to a favourable orientation for Michaelis complex formation with an optimized ligand. Differences in the conformational energies (ΔE) of a molecule after and before MM+ optimization (Table 6) within the partially flexible binding site showed that active compounds may form a Michaelis complex with suitable d_1 and α (see optimized values) without strong distortion of their optimal molecular geometry, as indicated by relatively low average ΔE value (7.59 ± 4.49 kcal/mol). In addition, geometric rearrangement for these compounds did not lead to steric collisions between nonbonded atoms. Alternatively, geometry suitable for Michaelis complex formation with inactive molecules was not attainable starting from their docking poses because their penetration to

Table 7
Results of docking and subsequent molecular optimization for favourable poses in the binding site of HNE for selected active (**5c**, **6c**, **8a**, **8b**, **8d** and **13f**) and inactive (**14b-d**, **17b** and **19b**) compounds

No.	α (deg)		Distances (Å)					Molecular deformation, ΔE (kcal/mol)
	Docking	Optimization	Docking	Optimization				
			d_1	d_1	d_2	d_3	$L = d_{2,min} + d_3$	
Active								
5c	71	86	4.09	2.39	2.17/2.45	2.99	5.16	12.89
6c	70	81	3.27	2.32	1.95/2.52	2.77	4.72	0.32
8a	69	90	3.03	2.37	3.38/3.56	3.88	7.26	4.65
8b	60	82	3.11	2.40	2.21/2.47	3.00	5.21	10.40
8d	68	90	3.34	2.36	3.72/3.97	4.15	7.87	7.92
13f	65	87	4.07	2.39	2.17/2.45	3.01	5.18	9.38
Inactive								
14b	160	86	5.55	2.32	2.16/2.52	2.86	5.02	18.07
14c	139	90	6.74	2.40	2.88/3.76	3.31	6.19	18.36
14d	147	85	4.55	2.36	3.21/3.34	3.58	6.79	18.70
17b	140	69	7.08	2.49	3.76/3.94	4.94	8.70	32.90
19b	156	88	5.65	2.39	3.05/4.62	4.72	7.77	26.50

Ser195 under the forces of harmonic restraints led to dramatic molecular distortion characterized by $\Delta E = 22.91 \pm 6.61$ kcal/mol.

The sum of d_3 distance and shorter d_2 value, denoted here as L (Table 6), represents the length of the channel for synchronous proton transfer from Ser195 through His57 to Asp102. It should be noted that there were no significant differences in distance L between active and inactive compounds investigated, which is in contrast to HNE inhibitors with a benzoylpyrazole scaffold.[23] MM+ optimization of docked structures with the applied harmonic restraints led to noticeable rotation of His57, both for active indazoles **8a**, **8d** and inactive compounds **14c**, **14d**, **17b**, **19b**. These geometric changes can be explained by the bulkiness of the molecules. Unlike benzoylpyrazoles,[23] the indazole derivatives investigated here contain a fused benzene ring, and their stiff scaffolds cause conformational changes in the receptor residues during Michaelis complex formation. Thus, it can be concluded that effects of distortion energy ΔE of a docked molecule on subsequent formation of the Michaelis complex is the main factor influencing biological activity of the compounds.

4. Conclusions

Our data demonstrate that the *N*-benzoylindazole scaffold is an appropriate system for development of HNE inhibitors and that a benzoyl substituent to the cyclic amide at N-1 was fundamental for activity, in agreement with the potent *N*-benzoylpyrazoles previously described. Our results also showed that the inclusion of a methyl or methoxy substituent at the *meta* position of this benzoyl group was favorable for activity. Likewise, modification of the ester function at position 4 of the indazole demonstrated that compounds with a methyl ester at this position were the most active. The most active derivatives (**8a** and **8b**) were found to be competitive, pseudoirreversible inhibitors of HNE and were relatively specific for HNE and chymotrypsin, as compared to other serine proteases, including thrombin and urokinase. Docking studies with partial flexibility of His57, Asp102, and Ser195 residues showed that orientation of active compounds in the HNE binding site is suitable for the interaction between the hydroxyl group of Ser195 and the carbonyl group of the inhibitor molecule. Moreover, changes in conformational energy during Michaelis complex formation for inactive compounds were significantly higher than those for the active inhibitors investigated. Further studies are in progress to improve our knowledge of structure–activity relationships of HNE inhibitors with an *N*-benzoylindazole scaffold.

5. Experimental section

5.1. Chemistry

All melting points were determined on a Büchi apparatus and are uncorrected. ^{1}H NMR spectra were recorded with an Avance 400 instruments (Bruker Biospin Version 002 with SGU). Chemical shifts are reported in ppm, using the solvent as an internal standard. Extracts were dried over Na_2SO_4, and the solvents were removed under reduced pressure. Merck F-254 commercial plates were used for analytical TLC to follow reactions. Silica gel 60 (Merck 70-230 mesh) was used for column chromatography. Microanalyses were performed with a Perkin-Elmer 260 elemental analyzer for C, H, and N, and the results were within ±0.4% of the theoretical values, unless otherwise stated. Reagents and starting materials were commercially available.

5.1.1. General procedures for 3a–k, 3m, and 3q

To a cooled (0 °C) suspension of 1H-indazole-3-carboxylic acid phenylamide **2**[34] (0.42 mmol) and a catalytic amount of Et_3N (0.05 mL) in anhydrous CH_2Cl_2 (1–2 mL), the appropriate aroyl chloride (1.25 mmol) was added. The mixture was stirred for 1–2 h at 0 °C and then for 1–3 h at room temperature. The precipitate was filtered off, and the solvent was evaporated *in vacuo*. Cold water (20 mL) was added, the mixture was neutralized with 0.5 N NaOH, and the precipitate was recovered by vacuum filtration. For compounds **3c**, **3e–f**, **3k**, and **3q**, the reaction mixture was extracted with CH_2Cl_2 (3 × 15 mL) after dilution. The solvent was dried over sodium sulphate to obtain the desired final compounds. Compound **3c** was purified by column chromatography using toluene/ethyl acetate 8:2 as eluent.

5.1.1.1. 1-Benzoyl-1H-indazole-3-carboxylic acid phenylamide, 3a. Yield = 29%; mp = 142–143 °C (EtOH); ^{1}H NMR ($CDCl_3$) δ 7.20 (t, 1H, Ar, J = 7.6 Hz), 7.40 (t, 2H, Ar, J = 7.6 Hz), 7.55–7.65 (m, 3H, Ar), 7.70 (m, 4H, Ar), 8.10 (m, 2H, Ar), 8.55 (m, 2H, Ar), 8.70 (exch br s, 1H, NH). Anal. ($C_{21}H_{15}N_3O_2$) C, H, N.

5.1.1.2. 1-(2-Methylbenzoyl)-1H-indazole-3-carboxylic acid phenylamide, 3b. Yield = 20%; mp = 129–130 °C (EtOH); ^{1}H NMR ($CDCl_3$) δ 2.45 (s, 3H, CH_3), 7.20 (m, 1H, Ar), 7.40 (m, 4H, Ar), 7.50–7.75 (m, 6H, Ar), 8.55 (s, 2H, Ar), 8.60 (exch br s, 1H, NH). Anal. ($C_{22}H_{17}N_3O_2$) C, H, N.

5.1.2. General procedures for 3l, 3o, and 3p

To a cooled and stirred solution of the appropriate acid (3-methoxybenzoic acid, thiophene 3-carboxylic acid and piperonylic acid) (0.42 mmol) and a catalytic amount of Et_3N (0.05 mL) in anhydrous DMF (1–2 mL), diethylcyanophosphonate (DCF) (1.68 mmol) and 1H-indazole-3-carboxylic acid phenylamide **2**[34] (0.42 mmol) were added. The mixture was stirred at room temperature for 12 h. After dilution with cold water, the suspension was extracted with CH_2Cl_2 (3 × 15 mL), and the solvent was evaporated *in vacuo*, resulting in a residue oil, which was purified by column chromatography using toluene/ethyl acetate (8:2) as eluent.

5.1.2.1. 1-(3-Methoxybenzoyl)-1H-indazole-3-carboxylic acid phenylamide, 3l. Yield = 15%; oil (purified by column chromatography using toluene/ethyl acetate 8:2 as eluent); ^{1}H NMR ($CDCl_3$) δ 3.95 (s, 3H, OCH_3), 7.15–7.25 (m, 2H, Ar), 7.40 (t, 2H, Ar, J = 8.0 Hz), 7.50 (t, 1H, Ar, J = 8.0 Hz), 7.55 (t, 1H, Ar, J = 7.6 Hz), 7.60 (s, 1H, Ar), 7.65–7.75 (m, 4H, Ar), 8.55 (d, 2H, Ar, J = 8.4 Hz), 8.70 (exch br s, 1H, NH). Anal. ($C_{22}H_{17}N_3O_3$) C, H, N.

5.1.2.2. 1-(Thiophene-3-carbonyl)-1H-indazole-3-carboxylic acid phenylamide, 3o. Yield = 21%; mp = 186–187 °C (EtOH); ^{1}H NMR ($CDCl_3$) δ 7.20 (t, 1H, Ar, J = 7.6 Hz), 7.40–7.50 (m, 3H, Ar), 7.55 (t, 1H, Ar, J = 8.0 Hz), 7.70 (t, 1H, Ar, J = 7.6 Hz), 7.75 (d, 2H, Ar, J = 7.6 Hz), 7.95 (d, 1H, Ar, J = 5.2 Hz), 8.55 (d, 1H, Ar, J = 8.0 Hz), 8.60 (d, 1H, Ar, J = 8.4 Hz), 8.65 (s, 1H, Ar), 8.75 (exch br s, 1H, NH). Anal. ($C_{19}H_{13}N_3O_2S$) C, H, N.

5.1.3. 1-(Pyridine-4-carbonyl)-1H-indazole-3-carboxylic acid phenylamide, 3n

Isonicotinic acid (0.42 mmol) was dissolved in $SOCl_2$ (0.7 mL) and refluxed for 1 h. After cooling, the excess of $SOCl_2$ was removed *in vacuo*, and the residue oil was dissolved in cold anhydrous toluene (3 mL). To this solution, a mixture of H-indazole-3-carboxylic acid phenylamide **2**[34] (0.42 mmol) and Et_3N (0.46 mmol) in 2.8 mL of anhydrous toluene was added. The mixture was stirred at 100 °C for 6 h. After cooling, the precipitate was recovered by vacuum filtration and washed with water, followed by 0.5 N NaOH, resulting in **3n**, which was recrystallized with ethanol. Yield = 21%; mp = 180 °C dec. (EtOH); ^{1}H NMR ($CDCl_3$) δ 7.20 (t, 1H, Ar, J = 7.6 Hz), 7.40 (t, 2H, Ar, J = 7.60 Hz), 7.60 (t, 1H, Ar, J = 8.0 Hz), 7.70 (d, 2H, Ar, J = 8.0 Hz), 7.75 (t, 1H, Ar, J = 8.4 Hz), 7.95 (d, 2H, Ar, J = 4.8 Hz), 8.55 (exch br s, 1H, NH), 8.60 (d, 2H, Ar, J = 8.4 Hz), 8.95 (d, 2H, Ar, J = 4.8 Hz). Anal. ($C_{20}H_{14}N_4O_2$) C, H, N.

5.1.4. General procedures for 5l, 5o, and 5p

Compounds **5l**, **5o**, and **5p** were obtained from 1H-indazole-3-carboxylic acid ethyl ester **4**[32] and the appropriate acid, following the same procedure described for **3l**, **3o** and **3p**. Compounds **5l** and **5o** were purified by column chromatography using toluene/ethyl acetate (8:2) as eluent, while compound **5p** was purified by crystallization from ethanol.

5.1.4.1. 1-(3-Methoxybenzoyl)-1H-indazole-3-carboxylic acid ethyl ester, 5l. Yield = 20%; mp = 81–83 °C (EtOH); ^{1}H NMR ($CDCl_3$) δ 1.50 (t, 3H, CH_2CH_3, J = 7.2 Hz), 3.90 (s, 3H, OCH_3), 4.55 (q, 2H, CH_2CH_3, J = 7.2 Hz), 7.20 (d, 1H, Ar, J = 8.8 Hz), 7.45 (t, 1H, Ar, J = 8.4 Hz), 7.55 (t, 1H, Ar, J = 7.2 Hz), 7.65–7.80 (m, 3H, Ar), 8.30 (d, 1H, Ar, J = 8.0 Hz), 8.60 (d, 1H, Ar, J = 8.8 Hz). Anal. ($C_{18}H_{16}N_2O_4$) C, H, N.

5.1.4.2. 1-(Thiophene-3-carbonyl)-1H-indazole-3-carboxylic acid ethyl ester, 5o. Yield = 14%; mp = 57–58 °C (EtOH); ^{1}H NMR ($CDCl_3$) δ 1.55 (t, 3H, CH_2CH_3, J = 7.2 Hz), 4.60 (q, 2H, CH_2CH_3, J = 7.2 Hz), 7.40 (d, 1H, Ar, J = 5.2 Hz), 7.50 (t, 1H, Ar, J = 7.6 Hz), 7.65 (t, 1H, Ar, J = 7.2 Hz), 8.00 (d, 1H, Ar, J = 5.2 Hz), 8.30 (d, 1H, Ar, J = 8.0 Hz), 8.60 (d, 1H, Ar, J = 8.4 Hz), 8.95 (s, 1H, Ar). Anal. ($C_{15}H_{12}N_2O_3S$) C, H, N.

5.1.5. General procedures for 5m, 5q, and 5r

Compounds **5m**, **5q** and **5r** were obtained from compound **4**,[32] following the general procedure described for **3a**–**k**, **3m** and **3q**. For compound **5m**, cold water (15 mL) was added after evaporation of the solvent, and the mixture was neutralized with 0.5 N NaOH. The precipitate was recovered by suction.

5.1.5.1. 1-(4-Cyanobenzoyl)-1H-indazole-3-carboxylic acid ethyl ester, 5m. Yield = 38%; mp = 140–142 °C (EtOH); ^{1}H NMR ($CDCl_3$) δ 1.50 (t, 3H, CH_2CH_3, J = 7.2 Hz), 4.55 (q, 2H, CH_2CH_3, J = 7.2 Hz), 7.55 (t, 1H, Ar, J = 8.0 Hz), 7.70 (t, 1H, Ar, J = 8.4 Hz), 7.85 (d, 2H, Ar, J = 8.4 Hz), 8.25 (d, 2H, Ar, J = 8.4 Hz), 8.30 (d, 1H, Ar, J = 8.0 Hz), 8.60 (d, 1H, Ar, J = 8.4 Hz). Anal. ($C_{18}H_{13}N_3O_3$) C, H, N.

5.1.5.2. 1-(Naphthalene-1-carbonyl)-1H-indazole-3-carboxylic acid ethyl ester, 5q. Yield = 28%; mp = 150–152 °C (EtOH); ^{1}H NMR ($CDCl_3$) δ 1.45 (t, 3H, CH_2CH_3, J = 7.2 Hz), 4.50 (q, 2H, CH_2CH_3, J = 7.2 Hz), 7.55–7.65 (m, 4H, Ar), 7.75 (m, 1H, Ar), 7.85 (d, 1H, Ar, J = 7.2 Hz), 7.95 (m, 1H, Ar), 8.05–8.15 (m, 2H, Ar), 8.30 (d, 1H, Ar, J = 8.0 Hz), 8.70 (d, 1H, Ar, J = 8.4 Hz). Anal. ($C_{21}H_{16}N_2O_3$) C, H, N.

5.1.6. General procedures for 5n and 5s

Compounds **5n** and **5s** were obtained from **4**[32] and the appropriate carboxylic acid, following the same procedure as described for **3n**. Compound **5n** was purified by column chromatography using CH_2Cl_2/MeOH 9.5:0.5 as eluent, and compound **5q** was recrystallized with ethanol.

5.1.6.1. 1-(Pyridine-4-carbonyl)-1H-indazole-3-carboxylic acid ethyl ester, 5n. Yield = 13%; mp = 119 °C dec. (EtOH); ^{1}H NMR ($CDCl_3$) δ 1.50 (t, 3H, CH_2CH_3, J = 7.2 Hz), 4.55 (q, 2H, CH_2CH_3, J = 7.2 Hz), 7.60 (t, 1H, Ar, J = 8.0 Hz), 7.75 (t, 1H, Ar, J = 7.6 Hz), 8.00 (d, 2H, Ar, J = 6 Hz), 8.30 (d, 1H, Ar, J = 8.0 Hz), 8.60 (d, 1H, Ar, J = 8.4 Hz), 8.90 (d, 2H, Ar, J = 6.0 Hz). Anal. ($C_{16}H_{13}N_3O_3$) C, H, N.

5.1.6.2. 1-(3,4,5-Trimethoxybenzoyl)-1H-indazole-3-carboxylic acid ethyl ester, 5s. Yield = 50%; mp = 160–163 °C (EtOH); ^{1}H NMR ($CDCl_3$) δ 1.50 (t, 3H, CH_2CH_3, J = 7.2 Hz), 3.95 (s, 6H, 2 OCH_3), 4.00 (s, 3H, OCH_3), 4.55 (q, 2H, CH_2CH_3, J = 7.2 Hz), 7.55 (t, 1H, Ar, J = 8.0 Hz), 7.60 (s, 2H, Ar), 7.70 (t, 1H, Ar, J = 8.4 Hz), 8.30 (d, 1H, Ar, J = 8.0 Hz), 8.60 (d, 1H, Ar, J = 8.4 Hz). Anal. ($C_{20}H_{20}N_2O_6$) C, H, N.

5.1.7. General procedures for 6b, 6c, and 6e

Compounds **6b**, **6c**, and **6e** were obtained from **4**[32] and the appropriate (cyclo)alkylchloride, following the same general procedure described for **3a**–**k**, **3m**, and **3q**. For these compounds, the mixtures were stirred at 0 °C for 2 h, and the solvent was evaporated *in vacuo*. Cold water was then added, the resulting suspensions were alkalinized with 0.5 N NaOH, and the precipitates were recovered by vacuum filtration.

5.1.7.1. 1-Propionyl-1H-indazole-3-carboxylic acid ethyl ester, 6b. Yield = 55%; mp = 101–103 °C (EtOH); ^{1}H NMR ($CDCl_3$) δ 1.40 (t, 3H, $COCH_2CH_3$, J = 7.2 Hz), 1.55 (t, 3H, OCH_2CH_3, J = 7.2 Hz), 3.40 (q, 2H, $COCH_2CH_3$, J = 7.2 Hz), 4.55 (q, 2H, OCH_2CH_3, J = 7.2 Hz), 7.50 (t, 1H, Ar, J = 8.0 Hz), 7.60 (t, 1H, Ar, J = 8.6 Hz), 8.25 (d, 1H, Ar, J = 8.0 Hz), 8.50 (d, 1H, Ar, J = 8.6 Hz). Anal. ($C_{13}H_{14}N_2O_3$) C, H, N.

5.1.7.2. 1-Butyryl-1H-indazole-3-carboxylic acid ethyl ester, 6c. Yield = 37%; mp = 57–59 °C (EtOH); ^{1}H NMR ($CDCl_3$) δ

1.10 (t, 3H, $CH_2CH_2CH_3$, J = 7.2 Hz), 1.55 (t, 3H, OCH_2CH_3, J = 7.2 Hz), 1.85–1.95 (m, 2H, $CH_2CH_2CH_3$, J = 7.2 Hz), 3.35 (t, 2H, $CH_2CH_2CH_3$, J = 7.2 Hz), 4.60 (q, 2H, OCH_2CH_3, J = 7.2 Hz), 7.50 (t, 1H, Ar, J = 8.0 Hz), 7.60 (t, 1H, Ar, J = 8.4 Hz), 8.25 (d, 1H, Ar, J = 8.0 Hz), 8.50 (d, 1H, Ar, J = 8.4 Hz). Anal. ($C_{14}H_{16}N_2O_3$) C, H, N.

5.1.8. 1-Cyclopentanecarbonyl-1H-indazole-3-carboxylic acid ethyl ester, 6d

Cyclopentanecarboxylic acid (0.525 mmol) dissolved in $SOCl_2$ (1 mL) was stirred at 100 °C for 1 h. After cooling, the excess $SOCl_2$ was removed *in vacuo*, and the residue was dissolved in cold anhydrous toluene (3–4 mL). To this solution, a mixture of 1H-indazole-3-carboxylic acid ethyl ester **4**[32] (0.525 mmol) and Et_3N (0.577 mmol) in toluene anhydrous (3 mL) was added, and the suspension was stirred at 110 °C for 5 h. After cooling, the precipitate was filtered off, the solvent was evaporated *in vacuo*, cold water (15 mL) was added, and resulting mixture was neutralized with 0.5 N NaOH and extracted with CH_2Cl_2 (3 × 15 mL). Evaporation of the solvent resulted in the final compound **6d**. Yield = 86%; oil; ^{1}H NMR ($CDCl_3$) δ 1.55 (t, 3H, OCH_2CH_3, J = 7.2 Hz), 1.75–1.85 (m, 4H, cC_5H_9), 1.95–2.05 (m, 2H, cC_5H_9), 2.10–2.20 (m, 2H, cC_5H_9), 4.20–4.30 (m, 1H, cC_5H_9), 4.60 (q, 2H, OCH_2CH_3, J = 7.2 Hz), 7.50 (t, 1H, Ar, J = 8.0 Hz), 7.60 (t, 1H, Ar, J = 8.4 Hz), 8.25 (d, 1H, Ar, J = 8.0 Hz), 8.50 (d, 1H, Ar, J = 8.4 Hz). Anal. ($C_{16}H_{18}N_2O_3$) C, H, N.

5.1.9. 1H-Indazole-3-carboxylic acid 2,2,2-trifluoroethyl ester, 7d

A solution of indazole-3-carboxylic acid (1.85 mmol) **1** in 6 mL of $SOCl_2$ was refluxed for 8 h. After cooling, the excess $SOCl_2$ was removed *in vacuo*, and the residue was dissolved in 6 mL of dry toluene. To this mixture, a solution of trifluoroethanol (26.6 mmol) and of Et_3N (6.24 mmol) in anhydrous toluene (6 mL) was added, and the mixture was stirred at room temperature. After 8 h, the solvent was evaporated *in vacuo*, and cold water was added to the residue oil to form a precipitate, which was recovered by suction. Yield = 77%; mp = 183–185 °C (EtOH); ^{1}H NMR ($CDCl_3$) δ 4.85 (q, 2H, OCH_2CF_3, J = 8.4 Hz), 7.40 (t, 1H, Ar, J = 8.0 Hz), 7.55 (t, 1H, Ar, J = 8.4 Hz), 7.65 (d, 1H, Ar, J = 8.0 Hz), 8.20 (d, 1H, Ar, J = 8.4 Hz), 11.45 (exch br s, 1H, NH). Anal. ($C_{10}H_7F_3N_2O_2$) C, H, N.

5.1.10. General procedures for 8a, b, e, f, i, j, m, and n

Compounds **8a**, **b**, **e**, **f**, **i**, **j**, **m**, and **n** were obtained starting from **7a–d** (**7a–c**[35]) and the appropriate ethero(aryl) chloride following the general procedures described for **3a–k**, **3m**, and **3q**. For compounds **8a**, **8b**, and **8m**, the mixtures were stirred for 1–2 h at 0 °C and then for 12 h at room temperature. For compounds **8e**, **8f**, **8i**, and **8j**, the reactions were carried out at 60 °C for 4–5 h. The resulting precipitates were filtered off, the solvent was evaporated, cold water (20 mL) was added, and the mixtures were neutralized with 0.5 N NaOH. Compound **8a** was recovered by vacuum filtration, whereas compounds **8b**, **e**, **f**, **i**, **j**, **m**, and **n** were extracted with CH_2Cl_2 (3 × 15 mL), and the solvent was evaporated *in vacuo* to afford the desired final compounds, which were recrystallized from ethanol.

5.1.10.1. 1-Benzoyl-1H-indazole-3-carboxylic acid methyl ester, 8a.

Yield = 37%; mp = 115–117 °C (EtOH); ^{1}H NMR ($CDCl_3$) δ 4.10 (s, 3H, OCH_3), 7.55 (m, 3H, Ar), 7.65 (m, 2H, Ar), 8.15 (m, 2H, Ar), 8.30 (d, 1H, Ar, J = 8.0 Hz), 8.60 (d, 1H, Ar, J = 8.4 Hz). Anal. ($C_{16}H_{12}N_2O_3$) C, H, N.

5.1.10.2. 1-(3-Methylbenzoyl)-1H-indazole-3-carboxylic acid methyl ester, 8b.

Yield = 37%; mp = 109–110 °C (EtOH); ^{1}H NMR ($CDCl_3$) δ 2.50 (s, 3H, CH_3), 4.05 (s, 3H, OCH_3), 7.45 (m, 2H, Ar), 7.55 (t, 1H, Ar, J = 8.0 Hz), 7.70 (t, 1H, Ar, J = 8.4 Hz), 7.95 (d, 2H, Ar), 8.30 (d, 1H, Ar, J = 8.0 Hz), 8.60 (d, 1H, Ar, J = 8.4 Hz). Anal. ($C_{17}H_{14}N_2O_3$) C, H, N.

5.1.11. General procedures for 8c and 8d

Compounds **8c** and **8d** were obtained starting from 1H-indazole-3-carboxylic acid methyl ester **7a**[35] and the appropriate acid (3-methoxybenzoic acid and thiophene 3-carboxylic acid) following the same procedure described for **3l**, **3o**, and **3p**. In this case, the mixtures were stirred at room temperature for 24 h. After dilution with cold water, compound **8c** suspension was extracted with CH_2Cl_2 (3 × 15 mL), the solvent was evaporated *in vacuo*, and the residue oil was purified by column chromatography using toluene/ethyl acetate (8:2) as eluent. Compound **8d** was filtered and purified by crystallization from ethanol.

5.1.11.1. 1-(3-Methoxybenzoyl)-1H-indazole-3-carboxylic acid methyl ester, 8c.

Yield = 18%; mp = 112–116 °C (EtOH); ^{1}H NMR ($CDCl_3$) δ 3.90 (s, 3H, OCH_3), 4.05 (s, 3H, $COOCH_3$), 7.20 (d, 1H, Ar, J = 8.0 Hz), 7.45 (t, 1H, Ar, J = 8.0 Hz), 7.55 (t, 1H, Ar, J = 7.6 Hz), 7.70 (m, 2H, Ar), 7.75 (d, 1H, Ar, J = 7.6 Hz), 8.30 (d, 1H, Ar, J = 8.0 Hz), 8.60 (d, 1H, Ar, J = 8.4 Hz). Anal. ($C_{17}H_{14}N_2O_4$) C, H, N.

5.1.11.2. 1-(Thiophene-3-carbonyl)-1H-indazole-3-carboxylic acid methyl ester, 8d.

Yield = 25%; mp = 113–114 °C (EtOH); ^{1}H NMR ($CDCl_3$) δ 4.10 (s, 3H, OCH_3), 7.45 (m, 1H, Ar), 7.55 (t, 1H, Ar, J = 7.6 Hz), 7.65 (t, 1H, Ar, J = 8.0 Hz), 8.00 (d, 1H, Ar, J = 5.2 Hz), 8.30 (d, 1H, Ar, J = 8.0 Hz), 8.60 (d, 1H, Ar, J = 8.4 Hz), 8.95 (s, 1H, Ar). Anal. ($C_{14}H_{10}N_2O_3S$) C, H, N.

5.1.12. General procedures for 8g, h, k, l, o, and p

Compounds **8g**, **h**, **k**, **l**, **o**, and **p** were obtained from **7b**,[35] **7d**, and the appropriate carboxylic acid (3-methoxybenzoic acid and thiophene 3-carboxylic acid), following the same procedure described for **3n**, with the exception of compound **8h**, which was refluxed for 10 h. After cooling, the precipitates were filtered off, and the solvent was evaporated under vacuum. After addition of cold water (20 mL), the mixtures were extracted with CH_2Cl_2. Evaporation of the solvent resulted in the final compounds, which were purified by flash chromatography using cyclohexane/ethyl acetate (4:1) as eluent for compounds **8k** and toluene/ethyl acetate (8:2) for **8o**. Compounds **8g**, **8h**, **8l**, and **8p** were recrystallized from ethanol.

5.1.12.1. 1-(3-Methoxybenzoyl)-1H-indazole-3-carboxylic acid propyl ester, 8g.

Yield = 55%; mp = 93–94 °C (EtOH); ^{1}H NMR ($CDCl_3$) δ 1.10 (t, 3H, $CH_2CH_2CH_3$, J = 7.2 Hz), 1.90 (m, 2H, $CH_2CH_2CH_3$), 3.90 (s, 3H, OCH_3), 4.45 (t, 2H, $CH_2CH_2CH_3$, J = 6.8 Hz), 7.20 (d, 1H, Ar, J = 8.0 Hz), 7.45 (t, 1H, Ar, J = 8.0 Hz), 7.55 (t, 1H, Ar, J = 7.6 Hz), 7.70 (t, 1H, Ar, J = 8.0 Hz), 7.75 (s, 1H, Ar), 7.80 (d, 1H, Ar, J = 8.0 Hz), 8.30 (d, 1H, Ar, J = 8.4 Hz), 8.60 (d, 1H, Ar, J = 8.0 Hz). Anal. ($C_{19}H_{18}N_2O_4$) C, H, N.

5.1.12.2. 1-(Thiophene-3-carbonyl)-1H-indazole-3-carboxylic acid propyl ester, 8h.

Yield = 52%; mp = 61–62 °C (EtOH); ^{1}H NMR ($CDCl_3$) δ 1.15 (t, 3H, $CH_2CH_2CH_3$, J = 7.2 Hz), 1.95 (m, 2H, $CH_2CH_2CH_3$), 4.50 (t, 2H, $CH_2CH_2CH_3$, J = 6.8 Hz), 7.40 (m, 1H, Ar), 7.50 (t, 1H, Ar, J = 8.0 Hz), 7.65 (t, 1H, Ar, J = 8.4 Hz), 8.00 (d, 1H, Ar, J = 5.2 Hz), 8.30 (d, 1H, Ar, J = 8.0 Hz), 8.60 (d, 1H, Ar, J = 8.4 Hz), 8.95 (s, 1H, Ar). Anal. ($C_{16}H_{14}N_2O_3S$) C, H, N.

5.1.13. General procedures 12a–f

To a cooled (−5 °C) and stirred solution of 3-*tert*-butoxycarbonylamino benzoic acid (0.26 mmol), **10** (prepared from precursor **9**, as reported in literature[36]) in anhydrous THF (2 mL) and 0.91 mmol of Et_3N were added. After 30 min, the mixture was allowed to warm up to 0 °C, and ethyl chloroformate was added (0.29 mmol).

After 1 h, 0.52 mmol of the appropriate 1H-indazole (**2**, **4**, **7a–d**) were added, and the reaction was carried out at room temperature for 12 h. For compounds **12d** and **12e**, the mixtures were stirred at 50–60 °C for 5–10 h. The suspensions were concentrated *in vacuo*, diluted with cold water, neutralized with 0.5 N NaOH, and extracted with CH_2Cl_2 (3 × 15 mL). The solvent was evaporated to afford the desired final compounds, which were purified by column chromatography using toluene/ethyl acetate (8:2) as eluent.

5.1.13.1. [3-(3-Phenylcarbamoyl-indazole-1-carbonyl)-phenyl]-carbamic acid *tert*-butyl ester, 12a. Yield = 15%; mp = 75–78 °C (EtOH); ^{1}H NMR ($CDCl_3$) δ 1.45 (s, 9H, C(CH_3)$_3$), 6.65 (exch br s, 1H, *NH*COO), 7.15 (t, 1H, Ar, J = 7.6 Hz), 7.30–7.40 (m, 2H, Ar), 7.50–7.60 (m, 3H, Ar), 7.70 (t, 1H, Ar, J = 7.6 Hz), 7.75 (m, 2H, Ar), 7.85 (d, 1H, Ar, J = 7.6 Hz), 8.55–8.65 (m, 3H, Ar), 9.15 (exch br s, 1H, NH). Anal. ($C_{26}H_{24}N_4O_4$) C, H, N.

5.1.13.2. 1-(3-*tert*-Butoxycarbonylamino-benzoyl)-1H-indazole-3-carboxylic acid ethyl ester, 12b. Yield = 10%; oil; ^{1}H NMR ($CDCl_3$) δ 1.30 (t, 3H, CH_2CH_3, J = 7.2 Hz), 1.55 (s, 9H, C(CH_3)$_3$), 4.55 (q, 2H, CH_2CH_3, J = 7.2 Hz), 6.65 (exch br s, 1H, *NH*CO), 7.45–7.55 (m, 2H, Ar), 7.65 (t, 1H, Ar, J = 7.6 Hz), 7.80–7.90 (m, 2H, Ar), 8.05 (s, 1H, Ar), 8.30 (d, 1H, Ar, J = 7.6 Hz), 8.55 (m, 1H, Ar). Anal. ($C_{22}H_{23}N_3O_5$) C, H, N.

5.1.14. General procedures for 13a–f

A mixture of **12a–f** (0.043 mmol), trifluoroacetic acid (0.28 mL), and CH_2Cl_2 (1.72 mL) was stirred at room temperature for 3 h. After evaporation of the solvent, diethyl ether was added to the residue, and the precipitate was recovered by vacuum filtration.

5.1.14.1. 1-(3-Aminobenzoyl)-1H-indazole-3-carboxylic acid phenylamide, 13a. Yield = 35%; mp = 85–88 °C (EtOH); ^{1}H NMR (DMSO-d_6) δ 6.90 (d, 1H, Ar, J = 8.4 Hz), 7.15 (t, 1H, Ar, J = 7.2 Hz), 7.20–7.30 (m, 2H, Ar), 7.40 (m, 3H, Ar), 7.60 (t, 1H, Ar, J = 8.0 Hz), 7.75 (t, 1H, Ar, J = 8.4 Hz), 7.80 (m, 2H, Ar), 8.25 (d, 1H, Ar, J = 8.0 Hz), 8.45 (d, 1H, Ar, J = 8.4 Hz), 9.05 (exch br s, 2H, NH_2), 10.45 (exch br s, 1H, NH). Anal. ($C_{21}H_{16}N_4O_2$) C, H, N.

5.1.14.2. 1-(3-Aminobenzoyl)-1H-indazole-3-carboxylic acid ethyl ester, 13b. Yield = 80%; mp = 152–155 °C (EtOH); ^{1}H NMR (DMSO-d_6) δ 1.40 (t, 3H, CH_2CH_3, J = 7.2 Hz), 4.15 (q, 2H, CH_2CH_3, J = 7.2 Hz), 6.95 (s, 1H, Ar), 7.20–7.30 (m, 3H, Ar), 7.60 (t, 1H, Ar, J = 8.0 Hz), 7.75 (t, 1H, Ar, J = 7.2 Hz), 8.25 (d, 1H, Ar, J = 8.0 Hz), 8.40 (d, 1H, Ar, J = 8.4 Hz), 9.10 (exch br s, 2H, NH_2). Anal. ($C_{17}H_{15}N_3O_3$) C, H, N.

5.1.15. General procedures for 14a and 14b

To a cooled (0 °C) suspension of 1H-indazole-3-carboxylic acid phenylamide **2**[34] (0.25 mmol) and a catalytic amount of Et_3N (0.05 mL) in anhydrous CH_2Cl_2 (1–2 mL), 0.25 mmol of the appropriate sulfonyl chloride (tosyl chloride and 4-chlorobenzenesulfonyl chloride) were added. The mixture was stirred at room temperature for 3–5 h. The precipitate was filtered off, the solvent was evaporated under vacuum, and water was added to the residue. Finally, the mixture was neutralized with 0.5 N NaOH, and the precipitate obtained was filtered and recrystallized with ethanol.

5.1.15.1. 1-(Toluene-4-sulfonyl)-1H-indazole-3-carboxylic acid phenylamide, 14a. Yield = 72%; mp = 185–188 °C (EtOH); ^{1}H NMR ($CDCl_3$) δ 2.45 (s, 3H, Ar), 7.20 (t, 1H, Ar, J = 7.6 Hz), 7.25 (m, 2H, Ar), 7.45 (m, 3H, Ar), 7.65 (t, 1H, Ar, J = 7.6 Hz), 7.75 (d, 2H, Ar, J = 8.0 Hz), 7.90 (d, 2H, Ar, J = 8.4 Hz), 8.25 (d, 1H, Ar, J = 8.0 Hz), 8.45 (d, 1H, Ar, J = 8.4 Hz), 8.85 (exch br s, 1H, NH). Anal. ($C_{21}H_{17}N_3O_3S$) C, H, N.

5.1.15.2. 1-(4-Chlorobenzenesulfonyl)-1H-indazole-3-carboxylic acid phenylamide, 14b. Yield = 78%; mp = 190–193 °C (EtOH); ^{1}H NMR ($CDCl_3$) δ 7.20 (t, 1H, Ar, J = 7.6 Hz), 7.45 (m, 2H, Ar), 7.50 (m, 3H, Ar), 7.65 (m, 1H, Ar), 7.80 (d, 2H, Ar, J = 8.0 Hz), 7.95 (d, 2H, Ar, J = 8.4 Hz), 8.25 (d, 1H, Ar, J = 8.0 Hz), 8.45 (d, 1H, Ar, J = 8.4 Hz), 8.80 (exch br s, 1H, NH). Anal. ($C_{20}H_{14}ClN_3O_3S$) C, H, N.

5.1.16. 1-(4-Chlorobenzyl)-1H-indazole-3-carboxylic acid phenylamide, 14c

A mixture of 1H-indazole-3-carboxylic acid phenylamide **2**[34] (0.63 mmol), K_2CO_3 (1.97 mmol) and 4-chlorobenzyl chloride (1.1 mmol) in 2 mL of anhydrous DMF was stirred at 80 °C for 1 h. After cooling, the mixture was diluted with cold water and the precipitate recovered by vacuum filtration.

Yield = 52%; mp = 127–130 °C (EtOH); ^{1}H NMR ($CDCl_3$) δ 5.65 (s, 2H, CH_2Ar), 7.20 (m, 3H, Ar), 7.30–7.45 (m, 7H, Ar), 7.80 (d, 2H, Ar, J = 8.0 Hz), 8.50 (d, 1H, Ar, J = 8.0 Hz), 8.85 (exch br s, 1H, NH). Anal. ($C_{21}H_{16}ClN_3O$) C, H, N.

5.1.17. 1-(4-Chlorophenyl)-1H-indazole-3-carboxylic acid phenylamide, 14d

A mixture of activated, powdered 4A molecular sieves (700 mg), dry CH_2Cl_2 (8 mL), **2**[34] (0.63 mmol), 4-chlorobenzenboronic acid (1.26 mmol), $Cu(Ac)_2$ (0.94 mmol), and Et_3N (1.26 mmol) was stirred at room temperature for 3 h. After filtration of the molecular sieves, the organic layer was washed with water (3 × 20 mL), followed by 33% aqueous ammonia (3 × 5 mL). The organic phase was dried over sodium sulfate, and the solvent was evaporated *in vacuo* to afford the final compound **14d**, which was purified by column chromatography using toluene/ethyl acetate (9.9:0.1) as eluent. Yield = 15%; mp = 130–132 °C (EtOH); ^{1}H NMR ($CDCl_3$) δ 7.20 (t, 1H, Ar, J = 7.6 Hz), 7.40 (m, 3H, Ar), 7.55 (t, 1H, Ar, J = 8.0 Hz), 7.60 (m, 2H, Ar), 7.70–7.80 (m, 5H, Ar), 8.60 (d, 1H, Ar, J = 8.4 Hz), 8.95 (exch br s, 1H, NH). Anal. ($C_{20}H_{14}ClN_3O$) C, H, N.

5.1.18. 1-(2-Oxo-2-phenylethyl)-1H-indazole-3-carboxylic acid ethyl ester, 14e

A mixture of 1H-indazole-3-carboxylic acid ethyl ester **4**[32] (0.42 mmol), phenacyl bromide (0.42 mmol), and K_2CO_3 (1.26 mmol) in anhydrous acetone was stirred at room temperature for 6 h. After evaporation of the solvent, cold water was added, and the precipitate was recovered by vacuum filtration. Yield = 98%; mp = 92–95 °C (EtOH); ^{1}H NMR ($CDCl_3$) δ 1.50 (t, 3H, OCH_2CH_3, J = 7.2 Hz), 4.55 (q, 2H, OCH_2CH_3, J = 7.2 Hz), 6.00 (s, 2H, CH_2COPh), 7.35 (m, 2H, Ar), 7.45 (t, 1H, Ar, J = 7.6 Hz), 7.55 (t, 2H, Ar, J = 8.0 Hz), 7.70 (t, 1H, Ar, J = 7.6 Hz), 8.05 (d, 2H, Ar, J = 7.6 Hz), 8.30 (d, 1H, Ar, J = 8.0 Hz). Anal. ($C_{18}H_{16}N_2O_3$) C, H, N.

5.1.19. General procedure for 14f and 14g

A mixture of 1H-indazole-3-carboxylic acid ethyl ester **4**[32] (0.52 mmol) and the appropriate phenylisocyanide (4-chlorophenylisocyanide and 3-methoxyphenylisocyanide) in 2 mL of anhydrous THF was stirred at room temperature for 12–20 h. After evaporation of the solvent, the residue was purified by crystallization from ethanol.

5.1.19.1. 1-(4-Chlorophenylcarbamoyl)-1H-indazole-3-carboxylic acid ethyl ester, 14f. Yield = 73%; mp = 125–127 °C (EtOH); ^{1}H NMR ($CDCl_3$) δ 1.55 (t, 3H, OCH_2CH_3, J = 7.2 Hz), 4.55 (q, 2H, OCH_2CH_3, J = 7.2 Hz), 7.40 (d, 2H, Ar, J = 8.4 Hz), 7.50 (t, 1H, Ar, J = 8.0 Hz), 7.65 (m, 3H, Ar), 8.25 (d, 1H, Ar, J = 8.0 Hz), 8.50 (d, 1H, Ar, J = 8.4 Hz), 9.20 (exch br s, 1H, NH). Anal. ($C_{17}H_{14}ClN_3O_3$) C, H, N.

5.1.19.2. 1-(3-Methoxyphenylcarbamoyl)-1H-indazole-3-carboxylic acid ethyl ester, 14g. Yield = 74%; mp = 102–105 °C (EtOH); ^{1}H NMR ($CDCl_3$) δ 1.55 (t, 3H, OCH_2CH_3, J = 7.2 Hz), 3.90 (s, 3H, OCH_3), 4.55 (q, 2H, OCH_2CH_3, J = 7.2 Hz), 6.75 (d, 1H, Ar, J = 8.0 Hz), 7.25 (d, 1H, Ar, J = 7.6 Hz), 7.35 (t, 1H, Ar, J = 8.0 Hz), 7.40 (s, 1H, Ar), 7.45 (t, 1H, Ar, J = 8.0 Hz), 7.65 (t, 1H, Ar, J = 7.6 Hz), 8.25 (d, 1H, Ar, J = 8.0 Hz), 8.55 (d, 1H, Ar, J = 8.4 Hz), 9.20 (exch br s, 1H, NH). Anal. ($C_{18}H_{17}N_3O_4$) C, H, N.

5.1.20. (3-Methylindazol-1-yl)-*m*-tolyl-methanone, 17a

Compound **17a** was obtained from compound **16**[37] by reaction with *m*-toluoyl chloride, following the procedure described for **3a–k**, **3m**, and **3q**. After evaporation of the solvent, cold water was added to the residue, followed by neutralization with 0.5 N NaOH. The mixture was then extracted with ethyl acetate, and the solvent was evaporated *in vacuo* to afford the desired final compound **17a**. Yield = 20%; mp = 79–80 °C (EtOH); ^{1}H NMR ($CDCl_3$) δ 2.45 (s, 3H, Ph-CH_3), 2.60 (s, 3H, CH_3), 7.45 (m, 3H, Ar), 7.65 (t, 1H, Ar, J = 7.6 Hz), 7.70 (d, 1H, Ar, J = 8.4 Hz), 7.90 (m, 2H, Ar), 8.55 (d, 1H, Ar, J = 8.4 Hz). Anal. ($C_{16}H_{14}N_2O$) C, H, N.

5.1.21. (3-Methoxyphenyl)-(3-methylindazol-1-yl)-methanone, 17b

Compound **17b** was obtained from **16**[37] by reaction with 3-methoxybenzoic acid following the same procedure described for **3n**. After cooling, the solvent was evaporated under vacuum, cold water was added, and the mixture was neutralized with 0.5 N NaOH and extracted with CH_2Cl_2. Evaporation of the solvent resulted in **17b**. Yield = 10%; mp = 62–65 °C (EtOH); ^{1}H NMR ($CDCl_3$) δ 2.60 (s, 3H, CH_3), 3.90 (s, 3H, OCH_3), 7.15 (d, 1H, Ar, J = 8.0 Hz), 7.45 (m, 2H, Ar), 7.65 (t, 2H, Ar, J = 8.0 Hz), 7.70 (t, 2H, Ar, J = 8.4 Hz), 8.55 (d, 1H, Ar, J = 8.4 Hz). Anal. ($C_{16}H_{14}N_2O_2$) C, H, N.

5.1.22. 1-(3-Methylbenzoyl)-1H-indazole-3-carboxylic acid, 19b

A mixture of **5c** (0.357 mmol) and 6 N NaOH (8 mL) was stirred at 50 °C for 5 h. After cooling, the mixture was acidified with 6 N HCl, and the precipitate was recovered by vacuum filtration and recrystallized with ethanol. Yield = 20%; mp = 267–269 °C dec. (EtOH); ^{1}H NMR ($CDCl_3$) δ 2.35 (s, 3H, CH_3), 7.30 (t, 1H, Ar, J = 7.6 Hz), 7.35–7.45 (m, 3H, Ar), 7.65 (d, 1H, Ar, J = 8.4 Hz), 7.75 (m, 2H, Ar), 8.10 (d, 1H, Ar, J = 8.0 Hz), 13.80 (exch br s, 1H, 0H). Anal. ($C_{16}H_{12}N_2O_3$) C, H, N.

5.2. HNE inhibition assay

Compounds were dissolved in 100% DMSO at 5 mM stock concentrations. The final concentration of DMSO in the reactions was 1%, and this level of DMSO had no effect on enzyme activity. The HNE inhibition assay was performed in black flat-bottom 96-well microtiter plates. Briefly, a buffer solution containing 200 mM Tris–HCl, pH 7.5, 0.01% bovine serum albumin, and 0.05% Tween-20 and 20 mU/mL of HNE (Calbiochem) was added to wells containing different concentrations of each compound. The reaction was initiated by addition of 25 μM elastase substrate (*N*-methylsuccinyl-Ala-Ala-Pro-Val-7-amino-4-methylcoumarin, Calbiochem) in a final reaction volume of 100 μL/well. Kinetic measurements were obtained every 30 s for 10 min at 25 °C using a Fluoroskan Ascent FL fluorescence microplate reader (Thermo Electron, MA) with excitation and emission wavelengths at 355 and 460 nm, respectively. For all compounds tested, the concentration of inhibitor that caused 50% inhibition of the enzymatic reaction (IC_{50}) was calculated by plotting % inhibition versus logarithm of inhibitor concentration (at least six points). The data are presented as the mean values of at least three independent experiments with relative standard deviations of <15%.

5.3. Analysis of compound stability

Spontaneous hydrolysis of selected *N*-benzoylindazoles was evaluated at 25 °C in 0.05 M phosphate buffer, pH 7.3. Kinetics of *N*-benzoylindazole hydrolysis was monitored by measuring changes in absorbance spectra over the incubation time using a SpectraMax Plus spectrophotometer (Molecular Devices, Sunnyvale, CA).

5.4. Analysis of inhibitor specificity

Selected compounds were evaluated for their ability to inhibit various proteases in 100 μL reaction volumes at 25 °C. Analysis of chymotrypsin inhibition was performed in reaction mixtures containing 0.05 M Tris–HCl, pH 8.0, 30 nM human pancreas chymotrypsin (Calbiochem, San Diego, CA), test compounds, and 100 μM substrate (Suc-Ala-Ala-Pro-Phe-7-amino-4-methylcoumarin). Thrombin inhibition was evaluated in reaction mixtures containing 0.25 M sodium phosphate, pH 7.0, 0.2 M NaCl, 0.1% PEG 8000, 1.7 U/mL human plasma thrombin (Calbiochem), test compounds, and 20 μM substrate (benzoyl-Phe-Val-Arg-7-amino-4-methylcoumarin). Analysis of urokinase inhibition assay was performed in reaction mixtures containing 0.1 M Tris–HCl, pH 8.0, 30 U/mL human urine urokinase (Calbiochem), test compounds, and 30 μM substrate (benzyloxycarbonyl-Gly-Gly-Arg-7-amino-4-methylcoumarin). Enzyme activity was monitored at excitation and emission wavelengths of 355 and 460 nm, respectively. For all compounds tested, the concentration of inhibitor that caused 50% inhibition of the enzymatic reaction (IC_{50}) was calculated by plotting % inhibition versus logarithm of inhibitor concentration (at least six points), and the data are the mean values of at least three experiments with relative standard deviations of <15%.

5.5. Molecular modeling

For computer-assisted molecular modeling, we employed HyperChem, version 7.0 (Hypercube Inc., Waterloo, ON, Canada) and ArgusLab 4.0.1 (Planaria Software LLC, Seattle, WA). Molecular structures were first created and optimized by HyperChem with the use of the molecular mechanics MM+ force field. These structures were then subjected to docking computations by ArgusLab with AScore scoring functions[51] to find the lowest-energy binding modes. Flexibility of an inhibitor was accounted for around all rotatable bonds automatically identified by ArgusLab. The binding site of HNE was considered to be rigid in the docking procedure, and its geometry was obtained by downloading a crystal structure of HNE complexed with a peptide chloromethyl ketone inhibitor[43] from the Protein Data Bank (code 1HNE). Amino acid residues within 7 Å of any non-hydrogen atom of the inhibitor were regarded as belonging to the binding site, and 22 residues satisfied this condition (Phe41, Cys42, Ala55, His57, Cys58, Leu99B, Asp102, Val190, Cys191, Phe192, Gly193, Asp194, Ser195, Gly196, Ser197, Ala213, Ser214, Phe215, Val216, Arg217A, Gly218, and Tyr224). Although Ala56 is 8.3 Å away from the nearest inhibitor atom, we included Ala56 in the binding site to maintain continuous sequence from Ala55 to Cys58. We then removed the chloromethyl ketone inhibitor and co-crystallized water molecules to obtain the 23-residue model of the HNE binding site that was used for docking.

Binding modes found for each inhibitor within a 2 kcal/mol gap above the lowest-energy mode were examined for the potential to form a Michaelis complex between the hydroxyl group of Ser195 and the inhibitor's carbonyl group in amido moiety, and values of d_1 and α (Fig. 2) were determined for each docked compound. These modes were further optimized by molecular mechanics with the MM+ force field using HyperChem. During this optimization,

we varied torsion angles r_1–r_5 in Ser195, His57, and Asp102 and also applied harmonic restraints to d_1 and α. Energy terms for the restraints were calculated as $E_d = K_d(d_1 - 1.5)^2$ and $E_\alpha = K_\alpha(\alpha - 100^\circ)$,[3] where $K_d = 15$ kcal mol^{-1} Å^{-1} and $K_\alpha = 3$ kcal mol^{-1} deg^{-1}. These restraints served as driving forces to attain the conditions of Michaelis complex formation through simultaneous cooperative movements of key residues within the binding site. Again, values of d_1 and α were determined, as well as distances d_2 and d_3 (Fig. 2). The distance d_2 is measured between the NH hydrogen in the His57 imidazole ring and either one of the carboxylic oxygens in Asp102. It defines the proton transfer from the oxyanion hole.[52] The distance between the hydroxyl proton in Ser195 and the basic pyridine-type nitrogen in His57 is also important for this transfer. However, because of easy rotation of the hydroxyl about the C–O bond in Ser195, we measured d_3 between the oxygen in Ser195 and the basic nitrogen in His57 (Fig. 2).

Molecular mechanics optimization of a binding mode also caused deformation of the molecule under investigation, and the change in energy (ΔE) due to deformation was calculated as $\Delta E = E_2 - E_1$, where E_1 is the MM+ conformational energy of the inhibitor molecule in the docked structure chosen as the favourable binding mode and where E_2 is the conformational energy of the inhibitor in its geometry attained after optimization of the docked structure under harmonic restrains.

Acknowledgements

This work was supported in part by National Institutes of Health grant P20 RR-020185 and the Montana State University Agricultural Experimental Station.

Supplementary data

Supplementary data (^{1}H NMR spectral data for derivatives **3c–k**, **3m**, **3p**, **3q**, **5p**, **5s**, **6e**, **8e**,**f**, **8i–p**, **12c–f**, and **13c–f** and elemental analyses for all final new compounds) associated with this article can be found, in the online version, at doi:10.1016/j.bmc.2011.06.036.

References and notes

1. Heutinck, K. M.; ten Berge, I. J.; Hack, C. E.; Hamann, J. *Mol. Immunol.* **2010**, *47*, 1943.
2. Sihna, S.; Watorek, W.; Karr, S.; Giles, J.; Bode, W.; Travis, J. *Proc. Natl. Acad. Sci. U.S.A.* **1987**, *84*, 2228.
3. Bode, W.; Meyer, E.; Powers, J. C. *Biochemistry* **1989**, *28*, 1951.
4. Chua, F.; Laurent, G. J. *Proc. Am. Thorac. Soc.* **2006**, *3*, 424.
5. Dollery, C. M.; Owen, C. A.; Sukhova, G. K.; Krettek, A.; Shapiro, S. D.; Libby, P. *Circulation* **2003**, *107*, 2829.
6. Bédard, M.; McClure, C. D.; Schiller, N. L.; Francoeur, C.; Cantin, A.; Denis, M. *Am. J. Respir. Cell Mol. Biol.* **1993**, *9*, 455.
7. Ficht, P. M.; Roghanian, A.; Howie, S. E.; Sallenave, J. M. *Biochem. Soc. Trans.* **2006**, *34*, 279.
8. Sifers, R. N. *Proc. Am. Thorac. Soc.* **2010**, *7*, 376.
9. Hiemstra, P. S. *Biochem. Soc. Trans.* **2002**, *30*, 116.
10. Mannino, D. M. *Semin. Resp. Crit. Care Med.* **2005**, *26*, 204.
11. Demkow, U.; van Overveld, F. J. *Eur. J. Med. Res.* **2010**, *15*, 27.
12. Straubaugh, S. D.; Davis, P. B. *Clin. Chest Med.* **2007**, *28*, 279.
13. Abboud, R. T.; Vimalanathan, S. *Int. J. Tuberc. Lung Dis.* **2008**, *12*, 361.
14. Henriksen, P. A.; Sallenave, J. *Int. J. Biochem. Cell Biol.* **2008**, *40*, 1095.
15. Chughtai, B.; O'Riordan, T. G. *J. Aerosol Med.* **2004**, *17*, 289.
16. Hofman, P. M. *World J. Gastroenterol.* **2010**, *14*, 5790.
17. Korkmaz, B.; Horwitz, M. S.; Jenne, D. E.; Gauthier, F. *Pharmacol. Rev.* **2010**, *62*, 726.
18. Bayer Healthcare Ag: WO2004020410 and WO2004020412; *Expert Opin. Ther. Patents* **2004**, *14*, 1511.
19. Ohbayashi, H. *Expert Opin. Invest. Drugs* **2002**, *11*, 965.
20. Abbenante, G.; Fairlie, D. P. *Med. Chem.* **2005**, *1*, 71.
21. Inoue, Y.; Omodani, T.; Shiratake, R.; Okazaki, H.; Kuromiya, A.; Kubo, T.; Sato, F. *Bioorg. Med. Chem.* **2009**, *17*, 7477.
22. Groutas, W. C.; Dou, D.; Alliston, K. R. *Expert Opin. Ther. Patents* **2011**, *21*, 339.
23. Schepetkin, I. A.; Khlebnikov, A. I.; Quinn, M. T. *J. Med. Chem.* **2007**, *50*, 4928.
24. Eilfeld, A.; Tabarro, C. M. G.; Frizler, M.; Sieler, J.; Schulze, B.; Gütschow, M. *Bioorg. Med. Chem.* **2008**, *16*, 8127.
25. Khlebnikov, A. I.; Schepetkin, I. A.; Quinn, M. T. *Bioorg. Med. Chem.* **2008**, *16*, 2791.
26. Mulchande, J.; Guedes, R. C.; Tsang, W.-Y.; Page, M. I.; Moreira, R.; Iley, J. *J. Med. Chem.* **2008**, *15*, 1783.
27. Li, Y.; Yang, Q.; Dou, D.; Alliston, K. R.; Groutas, W. C. *Bioorg. Med. Chem.* **2008**, *16*, 692.
28. Shreder, K. R.; Carica, J.; Du, L.; Fraser, A.; Hu, Y.; Kohno, Y.; Lin, E. C. K.; Liu, S. J.; Okerberg, E.; Pham, L.; Wu, J.; Kozarich, J. W. *Bioorg. Med. Chem. Lett.* **2009**, *19*, 4743.
29. Mulchande, J.; Oliveira, R.; Carrasco, M.; Gouveia, L.; Guedes, R. C.; Iley, J.; Moreira, R. *J. Med. Chem.* **2010**, *53*, 241.
30. Kawabata, K.; Suzuki, M.; Sugitani, M.; Imaki, K.; Toda, M.; Miyamoto, T. *Biochem. Biophys. Res. Commun.* **1991**, *177*, 814.
31. Iwata, K.; Doi, A.; Ohji, G.; Oka, H.; Oba, Y.; Takimoto, K.; Igarashi, W.; Gremillion, D. H.; Shimada, T. *Intern. Med.* **2010**, *49*, 2423.
32. Bistocchi, G. Alunni; De Meo, G.; Pedini, M.; Ricci, A.; Brouilhet, H.; Boucherie, S.; Rabaud, M.; Jacquignon, P. *Il Farmaco* **1981**, *36*, 315.
33. Lu, J.; Sheng, C.; Zhou, Y.; Zhu, J.; Zhang, W.; Zheng, C.; Zhu, J.; Zhang, J.; Lu, D.; Ning, W.; Zhang, X.; Ji, Y. Patent CN101239950, 2008.
34. Berdini, V.; Padova, A.; Saxty, G.; Woolford, A. J.-A.; Wyatt, P. G. Patent WO 2004014864 A1, 2004.
35. Shatalov, G. V.; Preobrazhenskii, S. A.; Mikhant'ev, B. I. *Izvestiya Vysshikh Uchebnykh Zavedenii, Khimiya I Khimicheskaya Teknologiya* **1978**, *21*, 656.
36. Mu, F.; Coffing, S. L.; Riese, D. J., II; Geahlen, R. L.; Verdier-Pinard, P.; Johnson, J.; Cushman, M. *J. Med. Chem.* **2001**, *44*, 441.
37. Lokhande, P. D.; Raheem, A.; Sabale, S. T.; Chabukswar, A. R.; Jagdale, S. C. *Tetrahedron Lett.* **2007**, *48*, 6890.
38. Auwers, K.; Kleiner, H. *J. Prak. Chem.* **1928**, *118*, 67.
39. Luisetti, M.; Piccioni, P. D.; Donnini, M.; Alesina, R.; Donnetta, A. M.; Peona, V. *Ann. N. Y. Acad. Sci.* **1991**, *624*, 343.
40. Shreder, K. R.; Cajica, J.; Du, L. L.; Fraser, A.; Hu, Y.; Kohno, Y.; Lin, E. C. K.; Liu, S. J.; Okerberg, E.; Pham, L.; Wu, J. Y.; Kozarich, J. W. *Bioorg. Med. Chem. Lett.* **2009**, *19*, 4743.
41. Veale, C. A.; Bernstein, P. R.; Bryant, C.; Ceccarelli, C.; Damewood, J. R., Jr.; Earley, R.; Feeney, S. W.; Gomes, B.; Cosmider, B. J.; Steelman, G. B. *J. Med. Chem.* **1995**, *38*, 98.
42. Walker, B.; Lynas, J. F. *Cell. Mol. Life Sci.* **2001**, *58*, 596.
43. Navia, M. A.; McKeever, B. M.; Springer, J. P.; Lin, T. Y.; Williams, H. R.; Fluder, E. M.; Dorn, C. P.; Hoogsteen, K. *Proc. Natl. Acad. Sci. U.S.A.* **1989**, 86.
44. Groutas, W. C.; Kuang, R.; Venkataraman, R.; Epp, J. B.; Ruan, S.; Prakash, O. *Biochemistry* **1997**, *36*, 4739.
45. Vergely, I.; Laugaa, P.; Reboud-Ravaux, M. *J. Mol. Graphics* **1996**, *14*, 145.
46. Aoyama, Y.; Uenaka, M.; Konoike, T.; Hayasaki-Kajiwara, Y.; Naya, N.; Nakajima, M. *Bioorg. Med. Chem. Lett.* **2001**, *11*, 1691.
47. Neumann, U.; Gutschow, M. *J. Biol. Chem.* **1994**, *34*, 21561.
48. Burgi, H. B.; Dunitz, J. D.; Lehn, J. M.; Wipff, G. *Tetrahedron* **1974**, *30*, 1563.
49. Dodson, G.; Wlodawer, A. *Trends Biochem. Sci.* **1998**, *23*, 347.
50. Katona, G.; Wilmouth, R. C.; Wright, P. A.; Berglund, G. I.; Hajdu, J.; Neutze, R.; Schofield, C. J. *J. Biol. Chem.* **2002**, *277*, 21962.
51. Morris, G. M.; Goodsell, D. S.; Halliday, R. S.; Huey, R.; Hart, W. E.; Belew, R. K.; Olson, A. J. *J. Comput. Chem.* **1998**, *19*, 1639.
52. Peters, M. B.; Merz, K. M. *J. Chem. Theory Comput.* **2006**, *2*, 383.